Universiteit Utrecht

Mathematical institute

DYNAMICAL SYSTEMS

Master's Thesis

July 2, 2020

The dynamics of the NE8 and NE9 systems, and predicting chaos

Caeser Abdulwahed
6045375

Supervision:

Prof. dr. F. (Ferdinand) Verhulst, Utrecht University

Examiners:

Prof. dr. Y. (Yuri) Kuznetsov, Utrecht University
Dr.P.A.(Paul) Zegeling, Utrecht University

Abstract

We considered the 3-dimensional systems of NE8 and NE9, which depend on a single non negative parameter a. We proved that in both systems, when $a = 0$ the systems have a line of equilibria in the $z-$axis and the eigenvalues and the behaviour of the eigenvectors indicate that the z^+-axis is an attractor. On the other hand, when $a > 0$ a periodic orbit in the neighbourhood of the origin appeared. The periodic orbit was revealed using the averaging method and represented analytically. However, when $a > 0$, in the NE9 system, nested tori appeared but were demolished at a range of initial values. Moreover, when a is small and the initial radius is large, a limit set and a chaotic attractor appeared. Furthermore, the existence of a chaotic attractor was shown numerically in the NE9 system. On the other hand, in the NE8 system, we proved analytically and showed numerically that the periodic orbit is an attractor and that several attractors appeared at different values of the parameter .

Contents

1 Introduction

Recently scholars have been interested in finding and studying systems of simple chaotic flows that do not contain equilibria [1, 6]. Little is known about the characteristics of such systems and systems that do not contain homoclinic or heteroclinic orbits [1]. Seventeen examples of these systems were listed in [2] and were given the following numbers: NE1 till NE17, which are nonlinear quadratic three dimensional systems with one parameter $a \geq 0$ [2]. Within this list, several systems, that have predicted a chaotic attractor, have been studied in details and the oldest and the best known of them is the conservative Sprott A (NE1) [1]. Recently, two other examples have been reported, which are the Wei (NE2) [6] and the Wang and Chen system (NE3) [5].

A systematic search has been done to find additional three dimensional chaotic systems with quadratic nonlinearities and no equilibria. The search was based on methods that were proposed in [7] using Matlab to find Lyapunov exponents and Kaplan-Yorke dimensions. Furthermore, we use two other methods for detecting chaos; the Poincare sections and the succession of period-doubling bifurcation limit cycles, which are not necessarily found in all systems. The seventeen systems were meant to be algebraically written in the simplest form which cannot be further reduced by the removal of terms without eliminating chaos [2]. The search was inspired by the observation that each of the known systems contains a constant term, which is an essential requirement for the absence of equilibrium points on one of the axes or at least one equilibrium point at the origin. Furthermore, when the constant is set to zero, the resulting system is nonhyperbolic (the equilibria have eigenvalues with a real part equal to zero), two of which are NE2 and NE3 [6, 5].

1.1 The NE8 and NE9 systems

The NE8 and NE9 systems have an axis of equilibria for $a = 0$, and they are described by these differential systems

$$\dot{x} = y \ , \ \dot{y} = -x - yz \ , \ \dot{z} = -xz + 7x^2 - a \quad (NE9)$$

$$\dot{x} = y \ , \ \dot{y} = -x - yz \ , \ \dot{z} = xy + 0.5x^2 - a \quad (NE8)$$

It has been determined that those systems contain chaotic behaviour depending on the sign of the Lyapunov exponents (LE), if the Kaplen-Yorke (D_{KY}) dimensions > 2. Chaotic behaviour appears in the NE8 system when the initial conditions are $a = 1.3$ and $(0, 0.1, 0)$, which produces an $LEs = 0.0314, 0, -10.2108$ and $D_{KY} = 2.0031$. As for NE9 system, the chaotic behaviour appears when the initial conditions are $a = 0.55$ and $(0.5, 0, 0)$, which produces an $LEs = 0.0504, 0, -0.3264$ and $D_{KY} = 2.15441$ [2].

Moreover, it has been determined that the NE8 and NE9 systems have similar dynamics to NE1, which is a special case of the Nose-Hoover oscillator [8] and a differential system that is given by the following equations, $\dot{x} = y \ , \ \dot{y} = -x - yz \ , \ \dot{z} = y^2 - a$, where $a \in \mathbb{R}$. The NE1 system has many engineering applications for predicting potential disastrous events that might occur in a structure such as a bridge [10]. Furthermore, the NE1 system has the following properties; For $a = 0$, the system has a line of equilibria in the $z-$axis and the phase space has a first integral, $f(x, y, z) = x^2 + y^2 + z^2$, which is a collection of concentric invariant spheres with two equilibrium points located at the south and north poles. The classification of these equilibrium points depends on the radius values of the spheres. However, for $a \neq 0$, the spheres are no longer invariant algebraic surfaces, and for $a > 0$ and small, the first order averaging theorem proves that the system has a stable periodic orbit in a neighbourhood of the origin corresponding to the initial values of $r_0 = \sqrt{2a}$, $z_0 = 0$. When the initial radius $r = \sqrt{x^2 + y^2}$ becomes slightly larger than the value of r_0, the motion becomes quasi periodic in which the orbit moves on a surface of a torus. However, when the radius increases to a certain value, the structure of the torus deforms and behaves chaotically as shown by the Poincare sections. Furthermore, it has been shown numerically that the system has a limit set for small values of the parameter a and large values of the initial radius, but when a increases the limit set evolves to a chaotic attractor. This was verified by calculating the Lyapunov exponents and the Kaplan-Yorke dimension at the initial values corresponding to the chaotic attractor and by numerically showing the sensitivity of the motion to the initial conditions.

However, some properties of the NE9 system remain unknown such as; the presence of a chaotic attractor and the way limit sets are formed. Moreover, there is an absence of an explicit application of the averaging method, which is the easiest method for finding a periodic orbit in the neighbourhood of the origin, and an analytical representation of the periodic orbit. As for the NE8, it remains unknown if the periodic orbit is an attractor, and what the shapes and number of limit cycles of the system are, as well as the type of chaotic behaviour that occurs in the system.

1.2 The Outline

For NE9 system, in section 2, we first explain the general behaviour of the system when $a \geq 0$, which includes the absence of any equilibrium points for $a > 0$ and that the value of the radius r and the variable z depend on the initial conditions. Furthermore for $a = 0$ we show how the phase space depends on the eigenvalues and the behaviour of eigenvectors. Subsequently, we apply the first and second order averaging method, which is the easiest method to find a stable periodic orbit and to illustrate the behaviour of the orbit in its neighbourhood, Afterwards we used The Poincare-Lindstedt method, which is the most commonly used method for providing a second order analytical representation of the orbit, and then compare between the analytical and the numerical solutions. Subsequently, we use the Poincare sections to confirm the results we found using the averaging method and show where the chaos starts. Furthermore, we show numerically how the limit set is formed and how it is changing to a chaotic attractor, and subsequently we examine the behavior of r and z during the formation of a limit set. At the end of the section, we show that the system behaves chaotically through a cascade of period doublings bifurcation limit cycles. As for system NE8, section 3, we give some properties of the system during the increase and the decrease of the orbit. Afterwards we apply the averaging theorem to the system, which showed that the system has a periodic solution and how the orbit behaves in the neighbourhood of the periodic orbit. Furthermore, we provide a second order analytical representation of the periodic orbit and show that the system has different limit cycles for different values of the parameter a. Finally, we show the chaotic behaviour of the system through a cascade of period doublings bifurcation limit cycles.

2 The NE9 System

The NE9 differential system is :

$$\dot{x} = y \ , \ \dot{y} = -x - yz \ , \ \dot{z} = -xz + 7x^2 - a, \tag{2.1}$$

where $a \in \mathbb{R}^+$ and the dot denotes the derivative with respect to the independent variable t. We show that assigning small positive values to the parameter a, which are considered as small perturbations to the system, leads to large changes in the behaviour of the system.

2.1 The general behaviour of the system for a small positive parameter

The changing rate of $r = \sqrt{x^2 + y^2}$ can be predicated from the relation:

$$\frac{d}{dt}(r^2) = \frac{d}{dt}(x^2 + y^2) = 2x\dot{x} + 2y\dot{y} = 2xy + 2y(-x - yz) = -2\dot{x}^2 z, \tag{2.2}$$

$$\frac{d}{dt}(r^2) = -2y^2 z. \tag{2.3}$$

From relation (2.3) we notice that r is decreasing when $z > 0$ and the decreasing rate of r increases when z increases in value as illustrated in Figure (1) for $a = 0$. In order to study the rotational behavior of the orbit we use the spherical coordinates:

$$x = R\sin\theta\cos\phi \ \ , \ \ y = R\sin\theta\sin\phi \ \ , \ \ z = R\cos\theta,$$

where R is the radial distance, ϕ is the azimuthal angle and θ is the polar angle, which can be redefined as

$$\begin{aligned}
\phi = \tan^{-1}(\frac{y}{x}) \Longrightarrow \dot{\phi} &= \frac{\dot{y}x - \dot{x}y}{x^2 + y^2} = -1 - \frac{xyz}{x^2 + y^2}, \\
\theta = \cos^{-1}(\frac{z}{R}) \implies \dot{\theta} &= \frac{-\dot{z}R + \dot{R}z}{R\sqrt{R^2 - z^2}}, \\
\dot{R} = \frac{x\dot{x} + y\dot{y} + z\dot{z}}{R} &= \frac{1}{R}(-y^2 z - xz^2 + 7x^2 z - az).
\end{aligned}$$

By substituting the spherical coordinates we get the following equations:

$$\begin{aligned}
&\dot{\phi} = -1 - R\cos\phi\sin\phi\cos\theta \ \ ; \ \ R = \sqrt{x^2 + y^2 + z^2}, \\
&\dot{\theta} = -R(\cos\theta\cos^2\phi + \cos\phi\cos\theta + \sin^2\phi\sin\theta\cos^2\theta - 7\cos^2\phi\sin\theta - 7\cos\phi\sin\theta\cos^2\theta) - \frac{a\cos^2\theta}{R\sin\theta}, \\
&\dot{R} = -R^2(\sin^2\theta\cos\theta\sin^2\phi + \cos^2\theta\sin\theta\cos\phi - 7\sin^2\theta\cos\theta\cos^2\phi) - a\cos\theta.
\end{aligned}$$

The first equation can be written in the form $\dot{\phi} = -1 - \frac{z}{2}\sin 2\phi$. This implies that for $-2 < z < 2$ the direction of the orbit's motion on the $xy-$plane is always clockwise and therefore the signs of x and y alternates during the motion,Figure (1). On the other hand, if $|z| > 2$ such that the inequality $z\sin 2\phi < -2$ is satisfied then ϕ reverses its direction and the motion becomes counterclockwise.

For the initial conditions $(x(0), y(0), z(0)) = (0, 0, z_0)$ we notice that the orbit stays on $z-$axis and that $z(t) = z(0) - at$, which implies that z is unbounded from below.

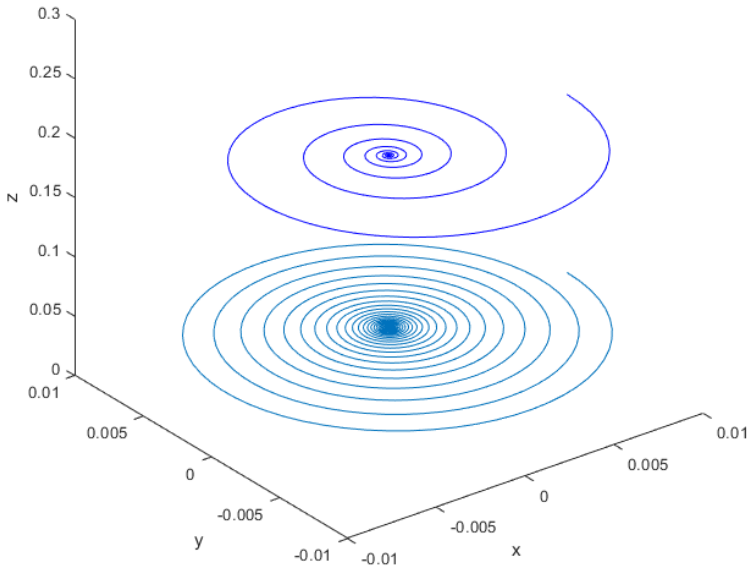

Figure 1: The decreasing rate of r is faster when z takes larger values. The initial points of the higher and lower orbits are $(0.01,0,0.2)$ and $(0.01,0,0.05)$ respectively and $a = 0$ for both cases. Here we have $|z| < 2$ is always satisfied during the motion.

The equation $\dot{z} = -xz + 7x^2 - a = 0$ represents a hyperbola in $xz-$plane, Figure (2a), and if the projection of the orbit on the plane is inside the branches of the hyperbola, then $\dot{z} < 0$, otherwise the apposite inequality occurs. On the other hand, when $2 > z > 0$ and a is small, the equation (2.3) implies that as r decreases, the maximum values of $|x|$ and $|y|$ also decreases during the rotation. Therefore, the inequality $\dot{z} = -xz + 7x^2 - a < 0$ becomes valid after a period of time, which corresponds to the projection of the orbit on $xz-$plane that is inside the hyperbola's branches. Meanwhile, z decreases until it becomes negative. When $z < 0$, equation (2.3) implies that the increase in r value increases the maximum value of the term $7x^2$, which increases the value of $\dot{z}$, that in turn makes the value of z increase until it becomes positive. These variables control the repetitive continuous behaviour of the orbit, which is illustrated in Figure (2a).

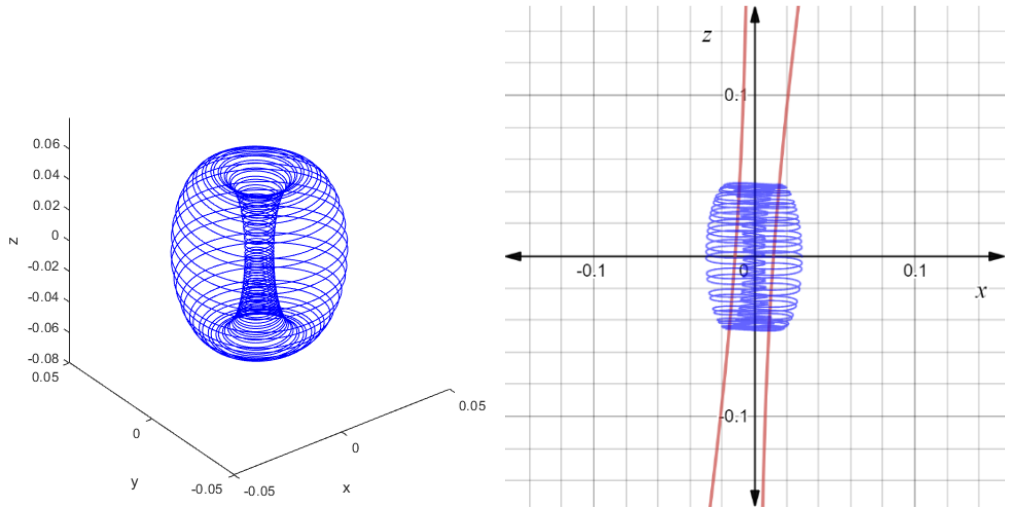

(a) (b)

Figure 2: (a) the orbit of the NE9 system, for $a = 0.001$ and the initial conditions $(0.03, 0, 0)$. (b) a plot of the third equation in (2.1) for $\dot{z} = 0$ and the same value of a, which is a hyperbola on the $xz-$ plane. The projection of the part of the orbit inside the hole on the $xz-$ plane is between the branches of the hyperbola.

Remark: It can be shown analytically, in case the initial point is not on $z-$axis, that the orbit can not be trapped inside the branches of the hyperbola where z is always decreasing. Furthermore, it will be shown in section (2.3) that the motion in Figure (2) is a quasi periodic one using the averaging method.

The motion of the orbit within the boundaries of the hyperbola and when z is bounded has the following dynamics: as r and z decrease, r approaches the z axis that leads to the decrease in its changing rate. This decrease in rate occurs because r is proportional to y^2 and z, while the changing rate of z becomes closer to the value of $-a$, as can be seen in equation (2.1) and it is larger than the changing rate of r. This implies that the orbit never intersects with the $z-$ axis and in general the motion follows the dynamic shown in Figure (2).

2.2 The behavior of the system for $a = 0$

2.2.1 The eigenvalues and eigenvectors of the system at equilibrium points

The equilibrium points of the system are the solutions to the following system of equations:

$$y = 0 \ , \ -x - yz = 0 \ , \ -xz - 7x^2 = 0.$$

This implies that the points of the form $(0, 0, z_0); z_0 \in \mathbb{R}$ are the equilibrium points of the system.

The Jacobian of the system is:

$$J = \begin{bmatrix} 0 & 1 & 0 \\ -1 & -z & -y \\ -z + 14x & 0 & -x \end{bmatrix} \Longrightarrow J|_{(0,0,z_0)} = \begin{bmatrix} 0 & 1 & 0 \\ -1 & -z_0 & 0 \\ -z_0 & 0 & 0 \end{bmatrix}.$$

By solving the equation $det(\lambda I - J) = 0 \ ; \ \lambda \in \mathbb{R}$, which is equivalent to the equations $\lambda(\lambda^2 + \lambda z_0 + 1) = 0$, we get

the following eigenvalues at $(0,0,z_0)$:

$$\lambda_1 = \frac{-z_0}{2} - \sqrt{\frac{z_0^2}{4} - 1} = \frac{-z_0}{2} - \frac{1}{2}\sqrt{z_0^2 - 4},$$
$$\lambda_2 = \frac{-z_0}{2} + \sqrt{\frac{z_0^2}{4} - 1}, = \frac{-z_0}{2} + \frac{1}{2}\sqrt{z_0^2 - 4},$$
$$\lambda_3 = 0.$$

Since we have at least one of the eigenvalues is zero then all the fixed points of the system are non hyperbolic. Moreover, if $z_0 > 0$, the real part of λ_1 and λ_2 is negative which implies that the positive z-axis is an attractor manifold. In addition, since the eigenvalues are complex, the orbit spirals around z_0 until it approaches a point on $z-$axis, in a neighbourhood of z_0. For $z_0 = 0$ the equilibrium point at the origin and the eigenvalues are 0 and $\pm 2i$, therefore the origin is an isolated zero-Hopf equilibrium point. When $z_0 > 2$, the phase flow converges faster to a point on $z-$axis in a neighbourhood of z_0. Figure (3) shows the three different cases where the initial point is in a neighbourhood of $z-$axis.

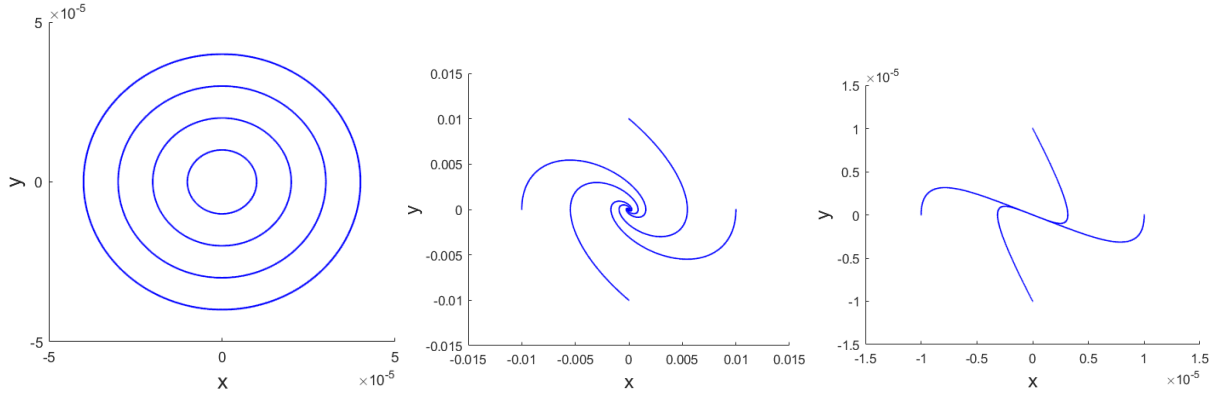

(a) (b) (c)

Figure 3: In all phase flows the four initial points are in a neighbourhood of $z-$axis and $a = 0$. (a) for $z_0 = 0$, the flow shows that the origin is a center. (b) we have $z_0 = 1$ where can see the rotation behaviour of the flow. Since the condition $|z| < 2$ is satisfied in both cases, the rotation of the motion is clockwise. (c) $z_0 = 2.5$, the flow has less rotational behaviour nearby $z-$axis.

The corresponding eigenvectors of λ_1, λ_2 and λ_3 are the solution to the linear system

$$(\lambda I - J)X = 0 \quad ; \quad X = (x, y, z).$$

Since the critical points of the system satisfy: $x = 0, y = 0, z = z_0; z_0 \in \mathbb{R}$, the corresponding system of λ_1 is:

$$y = x(\frac{-z_0}{2} - \frac{1}{2}\sqrt{z_0^2 - 4}),$$
$$-x - z_0 y = y(\frac{-z_0}{2} - \frac{1}{2}\sqrt{z_0^2 - 4}),$$
$$-z_0 x = z(\frac{-z_0}{2} - \frac{1}{2}\sqrt{z_0^2 - 4}).$$

The first and the second equations are identical and the third equation expresses z in terms of x. For $x = 1$, and after repeating the same process for λ_2 and λ_3 we find:

$$v_1 = (1, -\frac{1}{2}(z_0 + \sqrt{z_0^2 - 4}), \frac{2z_0}{z_0 + \sqrt{z_0^2 - 4}}) \ , \ v_2 = (1, \frac{1}{2}(-z_0 + \sqrt{z_0^2 - 4}), \frac{2z_0}{-z_0 + \sqrt{z_0^2 - 4}}) \ , \ v_3 = (0, 0, 1).$$

The presence of complex components of v_1 and v_2 indicates the local spiral nature of the behavior of the phase flow for $|z_0| < 2$, shown in Figure (3b).

2.2.2 The behavior of the orbit when $-2 < z < 0$

From the eigenvalues of the system we conclude that the phase flow is divergent when $z_0 < 0$ and then becomes convergent when the z component eventually becomes positive. Moreover, it can be shown that when $z < 0$ it eventually increases until it becomes positive. This implies that the orbit converges to a point on the positive part of $z-$axis as it is shown in Figure (4). However, when the initial points are symmetrical with respect to and in a neighbourhood of the origin, their corresponding orbits have the same limit.

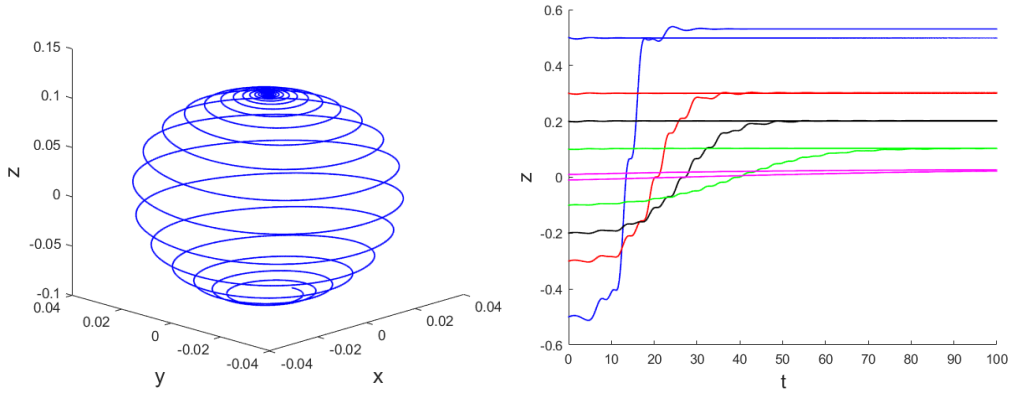

(a) (b)

Figure 4: For a negative value of z when $a = 0$. (a) the figure shows the behaviour of the orbit at the initial value $(x_0, y_0, z_0) = (0.01, 0, -0.1)$. The orbit shows that r and z increase until z becomes positive, after that r starts decreasing until the orbit approaches z axis. (b) the graph shows the limits the orbits for different initial values corresponding to some negative and positive values of z.

However, this property of the system becomes invalid when the initial radius increases, for example when $z_0 = \pm 0.5$, the limits of the two orbits would be slightly different from each other, as shown in Figure (4b). Furthermore, when the initial point is close to the origin, the changing rate of r becomes smaller, which leads the convergence to a critical point on $z-$axis to occur slower.

Subsequently, we use the averaging method to prove the existence of a periodic orbit in a neighbourhood of the origin, which was analytically represented using the Poincare-Lindstedt method. Afterwords, we use the Poincare sections to show the behavior of the orbit in the neighbourhood of the periodic orbit. In addition, we examine, in details, the chaotic attractor that the system has for some initial conditions, and then we numerically show the existence of period doubling limit cycles of the system at some initial conditions.

2.3 The first and the second order calculations using the averaging method

To prove the existence of a stable periodic orbit we use the first order averaging method and to obtain a more accurate approximation of the behaviour of the orbit in the neighbourhood of the periodic orbit we use the second order averaging method.

2.3.1 First order averaging

We show that the system has a stable periodic orbit in the neighbourhood of the origin by first rescaling the variables around the origin and then transferring the system to the polar coordinates (r, ψ, z). Afterwards, we average the trans-

ferred system and then determine the fixed points, and their types, of the averaged system. Finally, we scale the results according to the original system.

The first two equations in system (2.1) give:

$$\ddot{x} = \dot{y} = -x - yz \implies \ddot{x} + x = -\dot{x}z. \tag{2.4}$$

Then we make the following rescaling of the variables around the origin

$$x = \varepsilon\bar{x}\ ,\ \ y = \varepsilon\bar{y}\ \ ,\ \ z = \varepsilon\bar{z}\ \ ,\ \ a = \varepsilon^2 a_0. \tag{2.5}$$

Here we scaled the parameter a around zero of order (ε^2) for consistency.

Substituting (2.5) into (2.4) and in the expression of $\dot{z}$ of system (2.1), we get the following two equations, after leaving out the bars:

$$\begin{aligned} \ddot{x} + x &= -\varepsilon\dot{x}z, \\ \dot{z} &= \varepsilon(-xz + 7x^2 - a_0). \end{aligned} \tag{2.6}$$

For $\varepsilon \neq 0$ we assume that the first equation of system (2.6) has the solution

$$x = r\cos(t+\psi),\ \ \dot{x} = -r\sin(t+\psi). \tag{2.7}$$

Substitution of these expressions for x and $\dot{x}$ into the first equation of system (2.6) yields

$$-\dot{r}\sin(t+\psi) - r\cos(t+\psi)\dot{\psi} = -\varepsilon\dot{x}z. \tag{2.8}$$

From the form of the solution (2.7) we get

$$\frac{d}{dt}[r\cos(t+\psi)] = -r\sin(t+\psi),$$

which gives the following differential equation

$$\dot{r}\cos(t+\psi) - \dot{\psi}r\sin(t+\psi) = 0. \tag{2.9}$$

We consider (2.8) and (2.9) as two algebraic equations in $\dot{r}$ and $\dot{\psi}$, therefore the solution of the two equations is

$$\dot{r} = -\varepsilon r z\sin^2(t+\psi),\ \ \dot{\psi} = -\frac{1}{2}\varepsilon z\sin(2t+2\psi). \tag{2.10}$$

Averaging over z in system (2.6) leads to

$$\begin{aligned} \dot{z}_a &= \frac{1}{2\pi}\int_0^{2\pi} \varepsilon[7r_a^2\cos^2(t+\psi_a) - z_a r_a\cos(t+\psi_a) - a_0]dt \\ &= \frac{1}{2\pi}\int_0^{2\pi} \varepsilon(7r_a^2\frac{1+\cos(2t+2\psi_a)}{2} - a_0)dt \\ &= \varepsilon(\frac{7r_a^2}{2} - a_0), \end{aligned}$$

and averaging over r and ψ in system (2.10) leads to

$$\begin{aligned} \dot{r}_a &= \frac{1}{2\pi}\int_0^{2\pi} -\varepsilon r_a z_a\frac{1-\cos(2t+2\psi_a)}{2}dt = \frac{-\varepsilon r_a z_a}{2}, \\ \dot{\psi}_a &= \frac{1}{2\pi}\int_0^{2\pi} -\varepsilon z_a\frac{\sin(2t+2\psi_a)}{2}dt = 0 \implies \psi_a = \psi_0. \end{aligned}$$

So the averaging method produces the following system of ODEs:

$$\begin{aligned} \dot{r}_a &= \frac{-1}{2}\varepsilon r_a z_a, \\ \dot{\psi}_a &= 0, \\ \dot{z}_a &= \varepsilon(\frac{7r_a^2}{2} - a_0). \end{aligned} \tag{2.11}$$

It is clear that $(\sqrt{\frac{2a_0}{7}}, \psi_0, 0)$ is a critical point of the system. To find the initial values of a periodic solution we begin ,for example, with the following values $a_0 = 1, \varepsilon = 10^{-2}$ which leads to $a = 10^{-4}$ and $r_a = \sqrt{\frac{2a}{7}} = 0.0053452248$. Since $r_a = \sqrt{x^2+y^2}$ then $r_a = x$ when $y = 0$. This provided the required initial conditions for the periodic orbit, whose projections are shown in Figure (5).

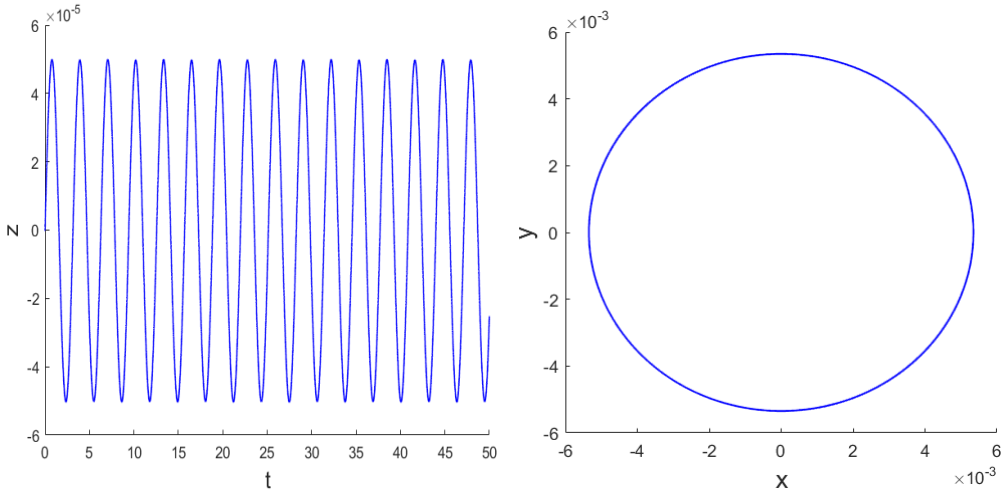

(a) (b)

Figure 5: (a) the projection of periodic solution on z-axis shows a small oscillation around $z = 0$ starting at $x(0) = 0.0053452248, y = 0, z = 0$ and $a = 10^{-4}$. (b) the graph shows the projection of the periodic solution on the $xy-$plane.

The Jacobian of the system at the critical point $(\sqrt{\frac{2a}{7}}, \psi_a, 0)$ is:

$$J|_{(\sqrt{\frac{2a}{7}}, \psi_a, 0)} = \begin{bmatrix} 0 & 0 & \frac{-1}{2}\varepsilon r_a \\ 0 & 0 & 0 \\ 7\varepsilon r_a & 0 & 0 \end{bmatrix}.$$

We notice that the rank of the Jacobian at the critical point equals 2. Moreover, the eigenvalues are given by the following equation

$$\det(\lambda I - J)|_{(\sqrt{\frac{2a}{7}}, \psi_a, 0)} = \begin{vmatrix} \lambda & 0 & \frac{1}{2}\varepsilon r_a \\ 0 & \lambda & 0 \\ -7\varepsilon r_a & 0 & \lambda \end{vmatrix} = \lambda \begin{vmatrix} \lambda & \frac{1}{2}\varepsilon r_a \\ -7\varepsilon r_a & \lambda \end{vmatrix} = \lambda(\lambda^2 + \frac{7}{2}\varepsilon^2 r_a^2) = 0,$$

and therefore we get the eigenvalues $\lambda_1 = 0$, $\lambda_{2,3} = \pm i\sqrt{\frac{7}{2}}\varepsilon r_a$. Since we have two purely imaginary eigenvalues we conclude that there exists an isolated Lyapunov stable 2π periodic solution in an $O(\varepsilon)$ neighbourhood of the origin as shown in Figure (5)

Remark: From the third equation in system (2.11) we conclude that z_a is always increasing in a neighbourhood of (ε) when $a = a_0 = 0$.

From the averaged system (2.11) we show, using the separation of variables, that the system has a first integral

$$\begin{aligned}
\frac{dr_a}{dz_a} &= \frac{-r_a z_a}{7r_a^2 - 2a_0} \\
\frac{7r_a^2 - 2a_0}{r_a} dr_a &= -z_a dz_a \\
(7r_a - \frac{-2a_0}{r_a}) dr_a &= -z_a dz_a \\
\frac{7r_a^2}{2} - 2a_0 \ln r_a &= -\frac{1}{2} z_a^2 + c \ \ ; \ \ c \in \mathbb{R}.
\end{aligned}$$

Therefore, the algebraic equations

$$\begin{aligned}
7r_a^2 - 4a_0 \ln r_a + z_a^2 &= c_1 \\
\psi_a &= \psi_0 \quad ; \quad c_1 \ , \ \psi_0 \in \mathbb{R},
\end{aligned}$$

represent a first integral of the averaged system (2.11), where the constants c_1 and ψ_0 are determined uniquely for some initial points and a value of a_0.

2.3.2 Second order averaging

The second order averaging method produces an approximation with higher precision than the first order, which might provide some qualitative features that might not be obtainable by the first order.

We apply the rescaling of the variables in the system (2.1) using the identities (2.5) and we obtain

$$\dot{x} = y \ \ , \ \ \dot{y} = -x - \varepsilon yz \ \ , \ \ \dot{z} = \varepsilon(-xz + 7x^2 - a_0), \tag{2.12}$$

Afterwards, we introduce the amplitude phase-variables $x(t) = r(t)\cos(t + \psi(t))$, $\dot{x}(t) = -r(t)\sin(t + \psi(t))$, and we get the following system:

$$\begin{aligned}
\dot{r} &= -\varepsilon r z \sin^2(t + \psi), \\
\dot{\psi} &= -\frac{1}{2} \varepsilon z \sin(2t + 2\psi), \\
\dot{z} &= \varepsilon(-rz\cos(t + \psi) + 7r^2 \cos^2(t + \psi) - a_0),
\end{aligned} \tag{2.13}$$

System (2.13) has the form $\dot{V} = \varepsilon f(t, V)$ where $V = (r, \psi, z)$ and

$$f(t, r, \psi, z) = \begin{bmatrix} -\frac{rz}{2} + \frac{rz}{2}\cos 2\alpha \\ -\frac{z}{2}\sin 2\alpha \\ -rz\cos\alpha + \frac{7}{2}r^2\cos 2\alpha + \frac{7}{2}r^2 - a_0 \end{bmatrix} \implies f^0(r, \psi, z) = \begin{bmatrix} -\frac{rz}{2} \\ 0 \\ \frac{7r^2}{2} - a_0 \end{bmatrix},$$

where $\alpha = t + \psi$. The gradient of f is:

$$\nabla f = \begin{bmatrix} -\frac{z}{2} + \frac{z}{2}\cos 2\alpha & -rz\sin 2\alpha & -\frac{r}{2} + \frac{r}{2}\cos 2\alpha \\ 0 & -z\cos 2\alpha & -\frac{1}{2}\sin 2\alpha \\ -z\cos\alpha + 7r\cos 2\alpha + 7r & rz\sin\alpha - 7r^2\sin 2\alpha & -r\cos\alpha \end{bmatrix},$$

and since the vector field is $u^1(t, x) = \int_0^t (f(s, x) - f^0(x))ds$, therefore

$$u^1 = \begin{bmatrix} \frac{rz}{4}\sin 2\alpha \\ \frac{z}{4}\cos 2\alpha \\ -rz\sin\alpha + \frac{7}{4}r^2\sin 2\alpha \end{bmatrix}.$$

We subsequently calculate $f^1 = \nabla f u^1$ and therefore

$$f^1 = \begin{bmatrix} -\frac{z}{2} + \frac{z}{2}\cos 2\alpha & -rz\sin 2\alpha & -\frac{r}{2} + \frac{r}{2}\cos 2\alpha \\ 0 & -z\cos 2\alpha & -\frac{1}{2}\sin 2\alpha \\ -z\cos\alpha + 7r\cos 2\alpha + 7r & rz\sin\alpha - 7r^2\sin 2\alpha & -r\cos\alpha \end{bmatrix} \begin{bmatrix} \frac{rz}{4}\sin 2\alpha \\ \frac{z}{4}\cos 2\alpha \\ -rz\sin\alpha + \frac{7}{4}r^2\sin 2\alpha \end{bmatrix}$$

$$= \begin{bmatrix} (-\frac{z}{2} + \frac{z}{2}\cos 2\alpha)(\frac{rz}{4}\sin 2\alpha) + (-rz\sin 2\alpha)(\frac{z}{4}\cos 2\alpha) + (-\frac{r}{2} + \frac{r}{2}\cos 2\alpha)(-rz\sin\alpha + \frac{7}{4}r^2\sin 2\alpha) \\ (-z\cos 2\alpha)(\frac{z}{4}\cos 2\alpha) + (-\frac{1}{2}\sin 2\alpha)(-rz\sin\alpha + \frac{7}{4}r^2\sin 2\alpha) \\ (-z\cos\alpha + 7r\cos 2\alpha + 7r)(\frac{rz}{4}\sin 2\alpha) + (rz\sin\alpha - 7r^2\sin 2\alpha)(\frac{z}{2}\cos 2\alpha) + (-r\cos\alpha)(-rz\sin\alpha + \frac{7}{4}r^2\sin 2\alpha) \end{bmatrix},$$

and after averaging we obtain:

$$f_1^0(r, \psi, z) = \begin{bmatrix} 0 \\ -\frac{z^2}{8} - \frac{7r^2}{16} \\ 0 \end{bmatrix}.$$

Therefore, we get a an $O(\varepsilon^2)$ system of the form

$$\dot{V} = \varepsilon f^0(V) + \varepsilon^2 f_1^0(V),$$

which can be written as

$$\begin{aligned} \dot{r}_a &= \frac{-\varepsilon rz}{2}, \\ \dot{\psi}_a &= -\varepsilon^2(\frac{z^2}{8} + \frac{7r^2}{16}), \\ \dot{z}_a &= \varepsilon(\frac{7r^2}{2} - a_0). \end{aligned}$$

We notice that $(\sqrt{\frac{2a_0}{7}}, \psi_0, 0)$ is a fixed point in the system of $O(\varepsilon)$. Afterwards, we calculate the Jacobian matrix of the last system and the eigenvalues at the fixed point.

$$J = \begin{bmatrix} \frac{-\varepsilon z}{2} & 0 & \frac{-\varepsilon r}{2} \\ -\frac{7\varepsilon^2 r}{8} & 0 & -\frac{\varepsilon^2 z}{4} \\ 7\varepsilon r & 0 & 0 \end{bmatrix} \implies J\big|_{(\sqrt{\frac{2a_0}{7}}, \psi_0, 0)} = \begin{bmatrix} 0 & 0 & -\frac{\varepsilon}{2}\sqrt{\frac{2a_0}{7}} \\ -\frac{\varepsilon^2}{8}\sqrt{\frac{2a_0}{7}} & 0 & 0 \\ 7\varepsilon\sqrt{\frac{2a_0}{7}} & 0 & 0 \end{bmatrix},$$

and therefore the characteristic equation is:

$$\lambda(\lambda^2 + \varepsilon^2 a_0) = 0,$$

which implies that either $\lambda_1 = 0$ or $(\lambda^2 + \varepsilon^2 a_0) = 0$ in which case $\lambda_{2,3} = \pm i\varepsilon\sqrt{a_0}$.

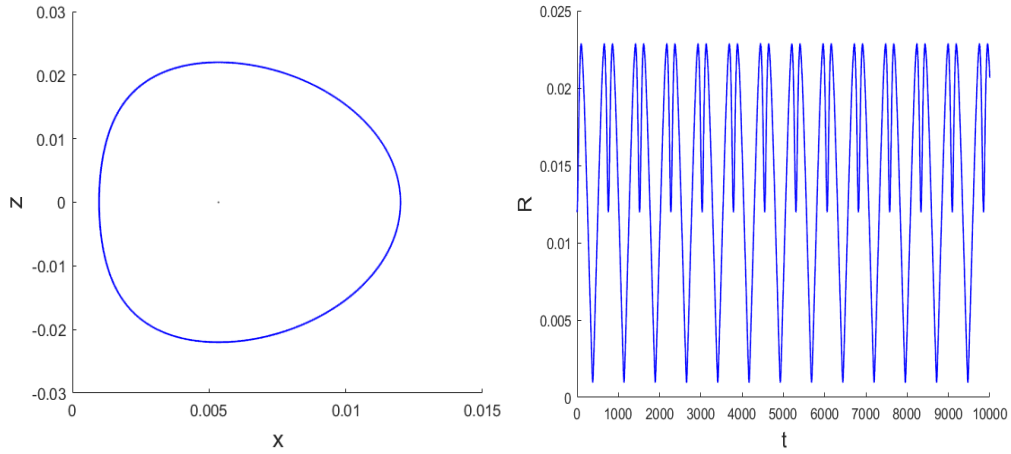

(a) (b)

Figure 6: (a) Poincare sections of an orbit for 10^5 time steps, that is constructed using the initial values of $a = 10^{-4}$, $(0.0053452248, 0, 0)$, and $(0.012, 0, 0)$ where the first initial point corresponds to the periodic orbit. (b) we see the oscillating value of $R = \sqrt{x^2 + y^2 + z^2}$, which corresponds to the second initial value and the same value of the parameter a.

Since the roots of the characteristic equation has two purely conjugate complex eigenvalues, we conclude that the orbit in a neighbourhood of the periodic orbit densely lays on a torus. Therefore, the motion of the orbit is a quasi periodic one, as shown in Figure (6a). A similar result was obtained using the first order approximation method. However, we notice that R shows a unique periodic behaviour, although the motion on the torus in not periodic, which occurs because of the horizontally-compressed shape of the torus. In Figure (6) we also notice that there is no damping in the amplitude of R which agrees with the result we obtained using the first and second averaging method, which implies that the periodic orbit is not an attractor.

2.4 The second order approximation of the periodic solution using The Poincare-Lindstedt method

In this section we show how to find convergent series approximations of the periodic solution. We stop at the second order approximation although continuing the process of calculation leads to an approximation of higher order of epsilon. The methods depends on expanding the variables around the origin, equating with respect to the order of epsilon, cancelling the secular terms, and applying the periodicity of the solutions.
The equations we get after re-scaling the variables are:

$$\begin{aligned} \ddot{x} + x &= -\varepsilon \dot{x} z, \\ \dot{z} &= \varepsilon(-xz + 7x^2 - \bar{a}). \end{aligned} \tag{2.14}$$

where the parameter is rescaled in the form $a = \varepsilon^2 \bar{a}$.

The first equation of system (2.14) has the form:

$$\ddot{x} + x = \varepsilon f(x, \dot{x}, z, \varepsilon) \;\; ; \;\; f(x, \dot{x}, z, \varepsilon) = -\dot{x} z. \tag{2.15}$$

We make the transformation:

$$\omega t = \theta \;\; ; \;\; \omega^{-2} = 1 - \varepsilon \eta(\varepsilon) \implies \frac{1}{\omega} = \sqrt{1 - \varepsilon \eta(\varepsilon)}.$$

The first and the second derivative with respect to θ are calculated as follows:

$$\theta = \omega t \implies \frac{d}{dt} = \frac{d\theta}{dt}\frac{d}{d\theta} = \omega\frac{d}{d\theta} \text{ and } \frac{d^2}{dt^2} = \omega^2\frac{d^2}{d\theta^2}.$$

We transform equation (2.15) using the notation $x' = \frac{dx}{d\theta}$ and we find that

$$x'' + x = \varepsilon[\eta x + (1-\varepsilon\eta)f(x,(1-\varepsilon\eta)^{\frac{-1}{2}}x', z, \varepsilon)], \tag{2.16}$$

$$\text{with initial values } x(0) = a(\varepsilon), x'(0) = 0. \tag{2.17}$$

By substituting in the equation (2.16) we obtain:

$$x'' + x = \varepsilon[\eta x - (1-\varepsilon\eta)^{\frac{1}{2}}x'z]. \tag{2.18}$$

The corresponding periodic solution of equation (2.18) can be represented by the convergent series:

$$x(\theta) = a(0)\cos\theta + \sum_{n=1}^{\infty}\varepsilon^n\gamma_n(\theta) \ , \ z(\theta) = z_0 + \sum_{n=1}^{\infty}\varepsilon^n z_n(\theta) \ ; \ z_0 = \text{constant}, \tag{2.19}$$

in which $\theta = \omega t = (1-\varepsilon\eta)^{\frac{-1}{2}}t$ while using the convergent series:

$$a = \sum_{n=0}^{\infty}\varepsilon^n a_n \ , \ \eta = \sum_{n=0}^{\infty}\varepsilon^n\eta_n \ , \ x(0) = a(0) + \sum_{n=1}^{\infty}\varepsilon^n\gamma_n(0) \ , \ 0 < \varepsilon \leq \varepsilon_0.$$

We have $\frac{1}{\omega} = \sqrt{1-\varepsilon\eta(\varepsilon)}$ and by using Taylor expansion of the function $\frac{1}{\omega}$ around $\varepsilon = 0$ we get:

$$\frac{1}{\omega} = 1 - \frac{1}{2}\varepsilon\eta_0 - \varepsilon^2(\frac{1}{2}\eta_1 + \frac{1}{8}\eta_0^2) + O(\varepsilon^3).$$

To determine $a(0)$ and $\eta(0)$ we substitute in the following equations:

$$\begin{aligned} \int_0^{2\pi}\sin\theta f(a(0)\cos\theta, -a(0)\sin\theta, z_0, 0)d\theta = 0, \\ \pi\eta(0)a(0) + \int_0^{2\pi}\cos\theta f(a(0)\cos\theta, -a(0)\sin\theta, z_0, 0)d\theta = 0. \end{aligned} \tag{2.20}$$

From the equation (2.15) we find that:

$$f(a(0)\cos\theta, -a(0)\sin\theta, z_0, 0) = a(0)z_0\sin\theta$$

After substituting in (2.20) we find that

$$\begin{aligned} \int_0^{2\pi}\sin\theta(a(0)z_0\sin\theta)d\theta = 0 \implies -\pi a(0)z_0 = 0, \\ \pi\eta(0)a(0) + \int_0^{2\pi}\cos\theta(a(0)z_0\sin\theta)d\theta = 0 \implies \pi\eta(0)a(0) = 0. \end{aligned} \tag{2.21}$$

From the second equation in system (2.14) we find that:

$$\omega z' = \varepsilon(-xz+7x^2-\bar{a}) \implies z(\theta) = \frac{1}{\omega}[z(0)+\int_0^\theta \varepsilon(-xz+7x^2-\bar{a})ds].$$

By using the expansion form of the variables we obtain:

$$\begin{aligned} z(\theta) &= \frac{1}{\omega}[z(0)+\varepsilon\int_0^\theta(-z_0a_0\cos s+7a_0^2\cos^2 s-\bar{a}+O(\varepsilon))ds], \\ &= \frac{1}{\omega}[z(0)+\varepsilon\int_0^\theta(-z_0a_0\cos s+\frac{7a_0^2}{2}(1+\cos 2s)-\bar{a}+O(\varepsilon))ds]. \end{aligned}$$

If z has a periodic solution then z has to be bounded. This requires cancelling secular terms in the last formula of z which implies that:

$$\frac{7a_0^2}{2}-\bar{a}=0 \implies a_0=\sqrt{\frac{2\bar{a}}{7}}. \tag{2.22}$$

Therefore, for $\bar{a}\neq 0$ we get $a_0=a(0)\neq 0$ and from the equations (2.21) we conclude that $z_0=\eta(0)=0$. Moreover, from equations (2.21) and equation (2.22) we get the system in a neighbourhood of $\varepsilon=0$

$$\begin{aligned} F_1(a,\eta,z_0) &= \frac{7a(0)^2}{2}-\bar{a}=0, \\ F_2(a,\eta,z_0) &= \pi\eta(0)a(0)=0, \\ F_3(a,\eta,z_0) &= -\pi a(0)z_0=0, \end{aligned}$$

which implies that the determinant of the Jacobian is:

$$|\frac{\partial(F_1,F_2,F_3)}{\partial(a(0),\eta(0),z_0)}| = \begin{vmatrix} 7a(0) & 0 & 0 \\ \pi\eta(0) & \pi a(0) & 0 \\ -\pi z_0 & 0 & -\pi a(0) \end{vmatrix} = -7\pi^2 a(0)^3 \neq 0, \tag{2.23}$$

therefore we conclude that there exists an isolated periodic solution which branches off for $\varepsilon>0$, which is the same result we obtained using the averaging theorem. Furthermore, since the condition (2.23) is satisfied, the periodic solution of (2.18) can be represented in the convergent series given in (2.19).

From the expansion form of η we get that $\eta_0=0$. Therefore, $\frac{1}{\omega}$ has the form:

$$\frac{1}{\omega}=1-\frac{1}{2}\varepsilon^2\eta_1+O(\varepsilon^3).$$

From the expansion form of $x(\theta)$ we find:

$$\begin{aligned} x(\theta) &= a(0)\cos\theta+\varepsilon\gamma_1(\theta)+\varepsilon^2\gamma_2(\theta)+..., \\ x'(\theta) &= -a(0)\sin\theta+\varepsilon\gamma_1'(\theta)+\varepsilon^2\gamma_2'(\theta)+..., \\ x''(\theta) &= -a(0)\cos\theta+\varepsilon\gamma_1''(\theta)+\varepsilon^2\gamma_2''(\theta)+.... \end{aligned}$$

By substituting in (2.18), knowing that $z_0=\eta_0=0$, we find that:

$$\begin{aligned} \varepsilon(\gamma_1''+\gamma_1)+\varepsilon^2(\gamma_2''+\gamma_2)+O(\varepsilon^3) = \varepsilon[&(\varepsilon\eta_1+\varepsilon^2\eta^2+O(\varepsilon^3))(a_0\cos\theta+\varepsilon\gamma_1+\varepsilon^2\gamma_2+O(\varepsilon^3))-(1-\frac{1}{2}\varepsilon^2\eta_1+O(\varepsilon^3)) \\ &\times(\varepsilon z_1+\varepsilon^2 z_2+O(\varepsilon^3))(-a_0\sin\theta+\varepsilon\gamma_1'+\varepsilon^2\gamma_2'+O(\varepsilon^3))]. \end{aligned}$$

By equating with respect to (ε^1) we obtain:

$$\gamma_1'' + \gamma_1 = 0,$$

which has a general solution of the form:

$$\gamma_1(\theta) = A_1 \cos\theta + B_1 \sin\theta.$$

The initial conditions state that the value of $A_1 = a_1$, and since $x'(0) = 0$, then $\gamma_1'(0) = 0$, which is substituted into the general solution, so $B_1 = 0$. Hence $\gamma_1(\theta) = a_1 \cos\theta$

By equating with respect to (ε^2) we find that:

$$\gamma_2'' + \gamma_2 = \eta_1 a_0 \cos\theta + z_1 a_0 \sin\theta. \tag{2.24}$$

To determine z_1 we apply the changing of the variables to the second equation in (2.14), so we get the equation:

$$\omega z' = \varepsilon(-xz + 7x^2 - \bar{a}) \implies z' = \frac{\varepsilon}{\omega}(-xz + 7x^2 - \bar{a}).$$

After writing the last equation in the expansion form knowing that $\eta_0 = z_0 = 0$ we get:

$$\begin{aligned}\varepsilon z_1' + \varepsilon^2 z_2' + \varepsilon^3 z_3' + O(\varepsilon^4) = \varepsilon(1 - \frac{1}{2}\varepsilon^2\eta_1 + O(\varepsilon^3))[-(a_0\cos\theta + \varepsilon\gamma_1(\theta) + \varepsilon^2\gamma_2(\theta) + O(\varepsilon^3)) \\ \times (\varepsilon z_1 + \varepsilon^2 z_2 + O(\varepsilon^3)) + 7(a_0\cos\theta + \varepsilon\gamma_1(\theta) + \varepsilon^2\gamma_2(\theta) + O(\varepsilon^3))^2 - \bar{a}].\end{aligned} \tag{2.25}$$

By equating both sides of $O(\varepsilon)$ we obtain:

$$\begin{aligned} z_1'(\theta) &= (7a_0^2\cos^2\theta - \bar{a}) = \frac{7}{2}a_0^2(1 + \cos 2\theta) - \bar{a} \implies \\ z_1(\theta) &= z_1(0) + \int_0^\theta [\frac{7}{2}a_0^2 - \bar{a} + \frac{7}{2}a_0^2\cos(2s)]ds, \end{aligned}$$

and since $\frac{7}{2}a_0^2 - \bar{a} = 0$, we get

$$z_1(\theta) = z_1(0) + \frac{7}{4}a_0^2\sin(2\theta) = z_1(0) + \frac{1}{2}\bar{a}\sin(2\theta).$$

Moreover, since $\int_0^{2\pi} z_1(\theta) = 0$ hence $z_1(0) = 0$, so we get $z_1(\theta) = \frac{1}{2}\bar{a}\sin(2\theta)$.

By substituting in (2.24) we get:

$$\begin{aligned}\gamma_2'' + \gamma_2 &= \eta_1 a_0\cos\theta + \frac{7}{4}a_0^3\sin(2\theta)\sin\theta = \eta_1 a_0\cos\theta - \frac{7}{8}a_0^3\cos(3\theta) + \frac{7}{8}a_0^3\cos(\theta) \\ &= a_0(\eta_1 + \frac{7}{8}a_0^2)\cos\theta - \frac{7}{8}a_0^3\cos(3\theta).\end{aligned}$$

The periodicity conditions implies that $\eta_1 + \frac{7}{8}a_0^2 = 0 \implies \eta_1 = -\frac{7}{8}a_0^2 = -\frac{1}{4}\bar{a}$ therefore we get:

$$\gamma_2'' + \gamma_2 = -\frac{7}{8}a_0^3\cos(3\theta).$$

The general solution to the last equation is:

$$\gamma_2(\theta) = A_2\cos\theta + B_2\sin\theta + \frac{7}{64}a_0^3\cos(3\theta).$$

From the initial conditions we find that $B_2 = 0$, $A_2 + \frac{7}{64}a_0^3 = a_2$.

To determine the constants a_1 and a_2 we find the formulas for z_2 and z_3, then we eliminate the secular terms. Afterwards, we equate with respect to (ε^2) and (ε^3) in (2.25) and we find:

$$\begin{aligned} z_2' &= -z_1 a_0 \cos\theta + 14 a_0 \gamma_1 \cos\theta = -\frac{7}{4}a_0^3 \cos\theta \sin 2\theta + 14 a_0 a_1 \cos^2\theta \\ &= -\frac{7}{8}a_0^3(\sin 3\theta + \sin\theta) + 7 a_0 a_1 + 7 a_0 a_1 \cos 2\theta. \end{aligned}$$

Cancelling secular terms requires that $a_1 = 0$, this means that $\gamma_1(\theta) = 0$. Therefore,

$$\begin{aligned} z_2(\theta) &= z_2(0) + \int_0^\theta -\frac{7}{8}a_0^3(\sin 3s + \sin s)ds \implies \\ z_2(\theta) &= z_2(0) + \frac{7}{24}a_0^3 \cos 3\theta + \frac{7}{8}a_0^3 \cos\theta - \frac{28}{24}a_0^3. \end{aligned}$$

Since we have $\int_0^{2\pi} z_2(\theta) = 0$, we find that $z_2(0) = \frac{28}{24}a_0^3 = \frac{7}{6}a_0^3$. Therefore we get:

$$z_2(\theta) = \frac{7}{24}a_0^3 \cos 3\theta + \frac{7}{8}a_0^3 \cos\theta.$$

By equating with respect to (ε^3) in (2.25) we get:

$$\begin{aligned} z_3' &= -\frac{1}{2}\eta_1(7a_0^2\cos^2\theta - \bar{a}) - z_2 a_0 \cos\theta + 14\gamma_2 a_0 \cos\theta \\ &= -\frac{1}{2}\eta_1(7a_0^2\cos^2\theta - \bar{a}) - a_0\cos\theta(\frac{7}{24}a_0^3\cos 3\theta + \frac{7}{8}a_0^3\cos\theta) + 14 a_0 \cos\theta(A_2\cos\theta + \frac{7}{64}a_0^3\cos 3\theta) \\ &= \frac{1}{2}(\frac{7}{2}\eta_1 a_0^2 - \frac{7}{8}a_0^4 + 14 a_0 A_2)(1+\cos 2\theta) - (\frac{7}{24}a_0^4 - \frac{49}{32}a_0^4)\cos 3\theta\cos\theta - \frac{1}{2}\eta_1\bar{a} \\ &= \frac{1}{2}(\frac{7}{2}\eta_1 a_0^2 - \frac{7}{8}a_0^4 + 14 a_0 A_2)(1+\cos 2\theta) - \frac{1}{2}(\frac{7}{24}a_0^4 - \frac{49}{32}a_0^4)(\cos 2\theta + \cos 4\theta) + \frac{1}{2}\eta_1\bar{a}. \end{aligned}$$

In order to cancel the secular terms we use the following condition:

$$\frac{1}{2}(-\frac{7}{2}\eta_1 a_0^2 - \frac{7}{8}a_0^4 + 14 a_0 A_2) + \frac{1}{2}\eta_1\bar{a} = 0 \implies A_2 = \frac{1}{16}a_0^3.$$

In conclusion, the second order approximation of the periodic solution is:

$$\begin{aligned} x(\theta) &= \sqrt{\frac{2\bar{a}}{7}}\cos\theta + \varepsilon^2[\frac{1}{16}(\frac{2}{7}\bar{a})^{\frac{3}{2}}\cos\theta - \frac{7}{64}(\frac{2}{7}\bar{a})^{\frac{3}{2}}\cos 3\theta] + O(\varepsilon^3), \\ y(\theta) &= -\sqrt{\frac{2\bar{a}}{7}}\sin\theta - \varepsilon^2[\frac{1}{16}(\frac{2}{7}\bar{a})^{\frac{3}{2}}\sin\theta - \frac{21}{64}(\frac{2}{7}\bar{a})^{\frac{3}{2}}\sin 3\theta] + O(\varepsilon^3), \\ z(\theta) &= \varepsilon\frac{1}{2}\bar{a}\sin(2\theta) + \varepsilon^2(\frac{2}{7}\bar{a})^{\frac{3}{2}}(\frac{7}{24}\cos 3\theta + \frac{7}{8}\cos\theta - \frac{7}{6}) + O(\varepsilon^3), \end{aligned} \tag{2.26}$$

after applying the Taylor expansion on ω we obtain the formula:

$$\omega = 1 + \frac{1}{2}\varepsilon\eta_0 + \varepsilon^2(\frac{1}{2}\eta_1 + \frac{3}{8}\eta_0^2) + O(\varepsilon^3).$$

Therefore, the expansion form of ω of the second order is:

$$\omega(\varepsilon) = 1 - \frac{1}{8}\bar{a}\varepsilon^2 + O(\varepsilon^3).$$

In Figure (5) we obtained a periodic solution to $O(\varepsilon)$ for the values $\varepsilon = 0.01$ and $\bar{a} = 1$. We compare this solution to the corresponding solution we obtained using the Poincare-Lindstedt method of the first and the second order of (ε), which were presented in the scaled formula of $z(\theta)$ in (2.26). However, the formula of the original coordinates have the form $\varepsilon(x(\theta), y(\theta), z(\theta))$ and $\varepsilon^2 \bar{a} = a$, which can be obtained by multiplying the formula of $z(\theta)$ in (2.26) by (ε), which yields

$$z(\theta) = \frac{1}{2} a \sin(2\theta) + 0.15272 a^{\frac{3}{2}} \left(\frac{7}{24}\cos 3\theta + \frac{7}{8}\cos\theta\right) + O(\varepsilon^3) \;\; ; \;\; a = 0.0001. \tag{2.27}$$

To compare the second order analytical solution with the numerical one we had using averaging method, Figure (5), both solutions should have the same initial point. This implies that $z(0) = 0$, which requires translating $z(\theta)$ in (2.27) by the amount $z = -0.15272 a^{\frac{3}{2}} \frac{28}{24} = 0,17817333333 a^{\frac{3}{2}}$. This implies that $z(\theta)$ becomes

$$z(\theta) = \frac{1}{2} a \sin(2\theta) + 0.15272 a^{\frac{3}{2}} \left(\frac{7}{24}\cos 3\theta + \frac{7}{8}\cos\theta\right) - 0.17817333333 a^{\frac{3}{2}} + O(\varepsilon^3) \;\; ; \;\; a = 0.0001. \tag{2.28}$$

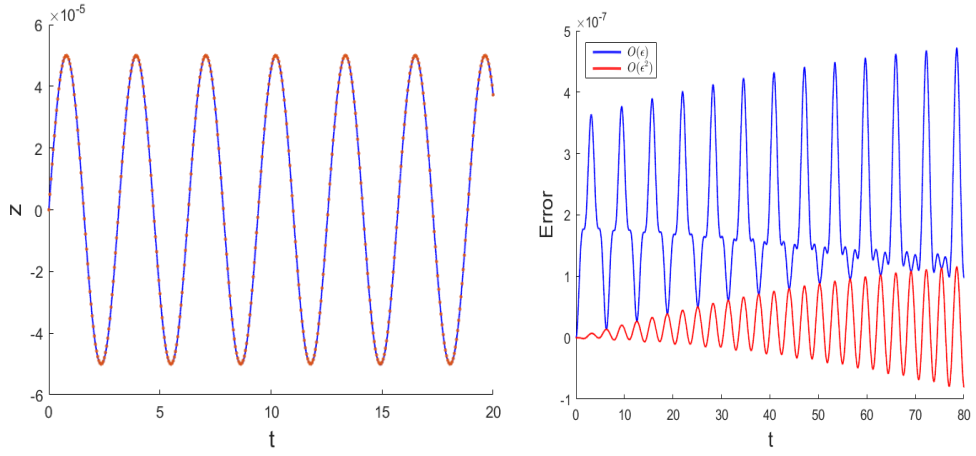

(a) (b)

Figure 7: (a) the periodic solution to $z(t)$ in the system NE9 that correspond to the initial point $(0.0053452248, 0, 0)$ and $a = 0.0001$. The solutions were obtained numerically (blue) and analytically (dotted red) of the order (ε). The two solutions seem to overlap almost perfectly on top of each other. (b) the errors of the first (blue) and the second order (red) of (ε) of the same periodic solution by Poincare-Lendstedt method. We used an $\varepsilon = 0.01$ and only the order (ε) of $z(\theta)$ in (2.26).

In Figure (7a), we compare the periodic solutions of $z(t)$ that was obtained by the averaging method (blue) and the first order approximation of $z(t) = \frac{1}{2} a \sin(2\theta)$ (red dotted). We find that up to the order (10^{-5}) the curves are almost identical, therefore if the curve of $O(\varepsilon^2)$ was plotted, it will not show a more accurate periodic solution to $z(t)$.

To examine the difference in accuracy between the first and the second order of approximation to the periodic solution with respect to (ε), we compare between the errors that occur while using the two methods. Figure (7b), shows that the error between the numerical solution and the analytical solution of the order $O(\varepsilon)$ (shown in blue) and the error between the numerical solution and the analytical solution of the order $O(\varepsilon^2)$ (shown in red) are both of the order (10^{-7}).

2.5 Poincare sections

In this section we use the Poincare sections on the system NE9 for different values of the parameter (a) to predict when the chaos in the system starts.

We have already proved the existence of a periodic solution of the system using the average theorem. The periodic solution is shown in Figure (8a, in black), which shows that any slight changes in the initial conditions changes the solution from a periodic to a quasi periodic one, which is an orbit that move on a torus. Moreover, the sequential changes in initial conditions produces nested tori, up to certain initial conditions, as shown in Figure (8a, in a variety of colors). However, there is no analytical proof of the existence of the nested tori around the periodic orbit.

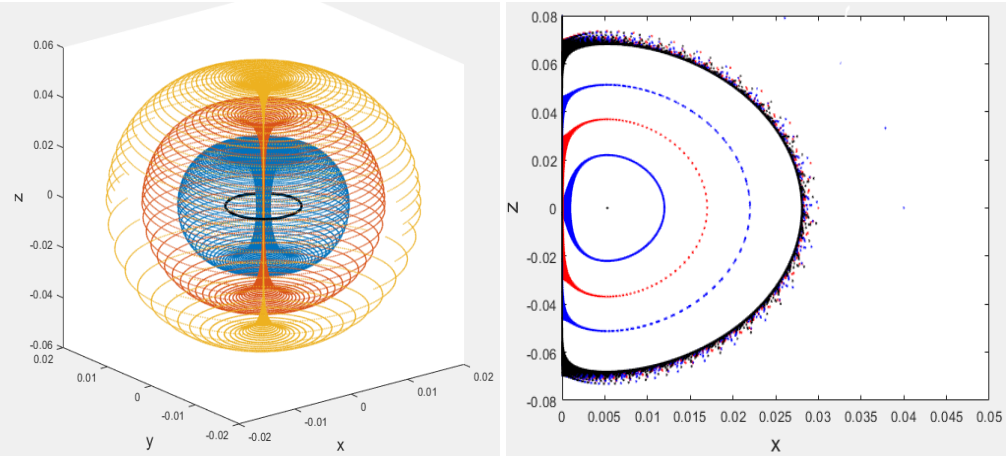

(a) (b)

Figure 8: (a) the orbits correspond to the initial values $(x_0,0,0)$ where x_0 takes the values [0.0053452248 , 0.012 , 0.017 , 0.022] and $a = 10^{-4}$, the first initial value correspond to the periodic solution. (b) Poincare sections that correspond to the same initial values in order except for the region where the chaos starts, it corresponds to the initial value $(\alpha,0,0)$ where α takes the values [0.4 , 0.5 , 0.6]. Here we assume $\varepsilon = 0.01$.

Up to certain initial conditions the behavior of the orbit continues until the surface of the torus is deformed and the chaotic motion appears. The behaviour of the periodic orbit at a variety of initial conditions is shown using Poincare sections that are shown in Figure (8b). These sections illustrate that when the chosen initial point is close enough to an initial point of the periodic solution, which corresponds to a dot in Poincare sections, the orbit moves on a surface of a torus. However, the region corresponding to the largest radius in Poincare sections is the region where chaos appears, which is a result of the deformation of the torus in which the orbit increases in density in a sub-region of the space.

The behaviour of the orbit described so far occurs when a is small, i.e. $a = 10^{-4}$, but when a increases it leads to a different behaviour shown in Figure (9). During periodic motion, the torus corresponding to the quasi periodic motion quickly deforms to create a series of islands as seen in Poincare section. Moreover, increasing the distance from the initial point, that corresponds to the periodic orbit, causes the orbit to behave chaotically as shown near the edges of the Figure (9) in blue.

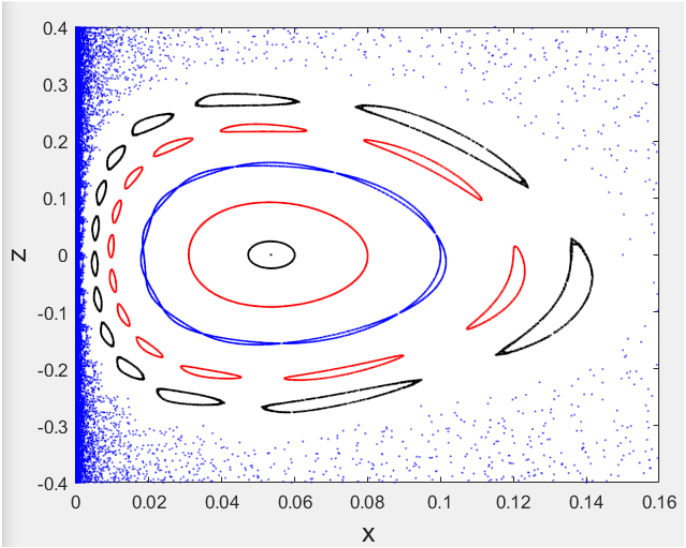

Figure 9: Poincare sections of a periodic orbit (black dot) followed by quasi periodic orbits (black and red orbits and other orbits that appear as islands in the section ,and then followed by the chaotic region in blue. All Poincare sections were made of orbits that were constructed when $a = 0.01$, $\varepsilon = 0.1$ and at the initial values $(x_0, 0, 0)$ where $x_0 = [0.053452248, 0.06, 0.08, 0.1, 0.12, 0.14, 0.15]$.

2.6 The formation of the chaotic attractor

When the orbit of the system, at some initial conditions, is bounded and continuously turning without repeating any of its turns, it is called a chaotic attractor such that its Kaplan-Yorke dimension is between 2 and 3.[7]

The averaging method shows that there is a stable periodic solution in a neighbourhood of the origin corresponding to $r_0 = \sqrt{\frac{2a}{7}}$ and $z_0 = 0$ for a is small. By increasing the initial radius, where a is fixed, the motion changes to a quasi periodic one where the orbit moves on a torus. However, during the increase of the initial radius the torus deforms at a particular value of the radius and the motion changes to chaotic as it is illustrated using Poincare sections. A limit set appears during the increase of the initial radius, where a is small. When a increases, the limit set evolves to a chaotic attractor as it is shown in Figure (10). For a stronger indication to the chaotic attractor we calculate Lyapunov exponents, and Kaplan and Yorke dimension. For the corresponding initial conditions of the chaotic attractor $a = 0.01$, $(0.2, 0, 0)$ we find $LE_1 = 0.02$, $LE_2 = 0$, $LE_3 = 0.218$.

The Kaplan and Yorke dimension is defined by: $D_L = j + \frac{1}{|\lambda_{L_{j+1}}|} \sum_{i=1}^{j} \lambda_{L_i}$ where j is the largest integer satisfying $\sum_{i=1}^{j} \lambda_{L_i} \geq 0$ and $\sum_{i=1}^{j+1} \lambda_{L_i} < 0$. Therefore, Kaplan-Yorke dimension corresponding to the chaotic attractor is $D_{KY} = 2.0914$, which is between 2 and 3, and therefore it satisfies a necessary condition of having a chaotic attractor in the system.

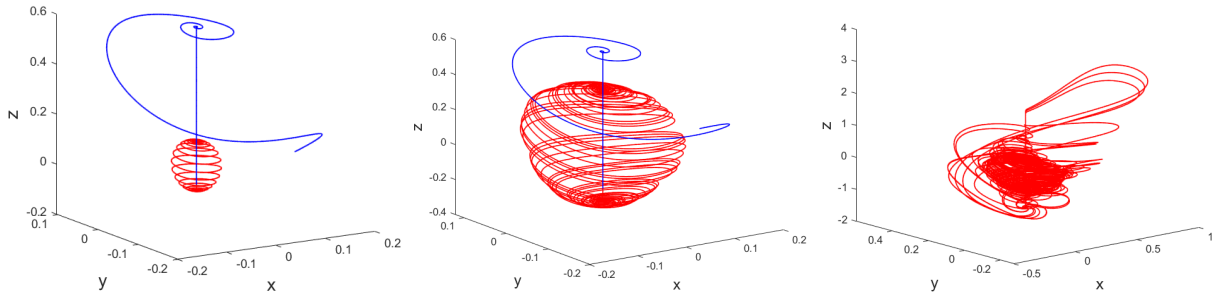

(a) (b) (c)

Figure 10: Three orbits illustrating transition from a limit set to a chaotic attractor for $a = 0.0001, 0.001, 0.01$ respectively and for the initial values $(0.2, 0, 0)$. (a) and (b) show how the limit set expands when a increases. However, the structure of the limit set demolishes as the parameter a increases to form a chaotic attractor as it is illustrated in (c).

Poincare section to the chaotic attractor shows how the orbit behaves in the chaotic attractor, which indicates that the orbit is dense in a confined region of the space, Figure (11)

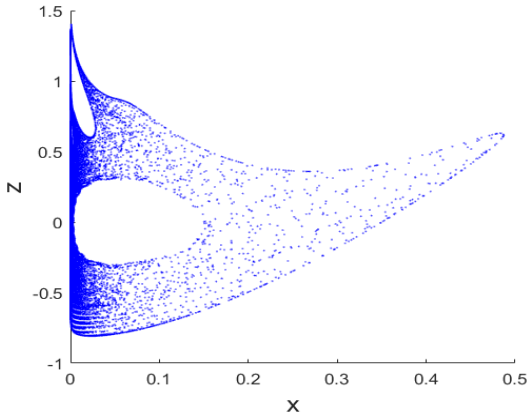

Figure 11: The Poincare section of the orbit for $a = 0.01$ and for the initial value $(0.2, 0, 0)$, which illustrates the density of the orbit in a sub-region of the space nearby the origin.

In Figure(12) the $x(t)$ components of two solutions of the system for $a = 0.01$, with very close initial points; $(0.0001, 0, 0)$ and $(0.000001, 0, 0)$ appear to diverge over time confirming the choatic behaviour of their orbits. Furthermore, for the same value of a, the Lyapunov exponents are $LE_1 = 0.03$, $LE_2 \approx 0$, $LE_3 = -3.337$.

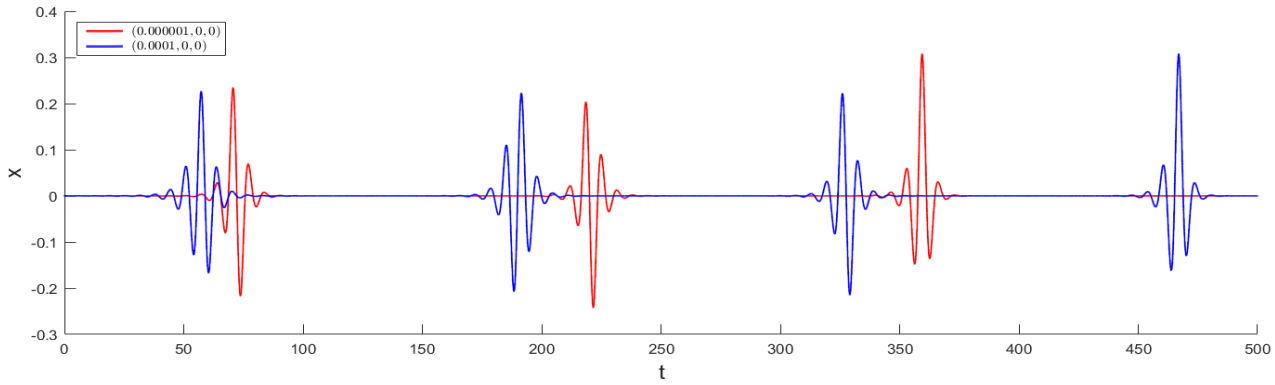

Figure 12: The change in $x(t)$ over time for $a = 0.01$ and for the very close initial points $(0.0001, 0, 0)$ (blue) and $(0.000001, 0, 0)$ (red). The plot illustrates the sensitivity of the solution to the initial condition of the system.

Furthermore, the sensitivity to initial conditions is predicted to occur even for larger values of the parameter a. For example, for $a = 0.1$ and for the very close initial points $(0.3, 0, 0)$ and $(0.30001, 0, 0)$ a divergence between $x(t)$ components of the solutions occurs, Figure (13). Moreover, the corresponding Lyapunov exponents are $LE_1 = 0.060363$, $LE_2 \approx 0$, $LE_3 = -3.209832$, which further indicates, at those initial conditions, the sensitivity of the motion of the orbit to the initial conditions.

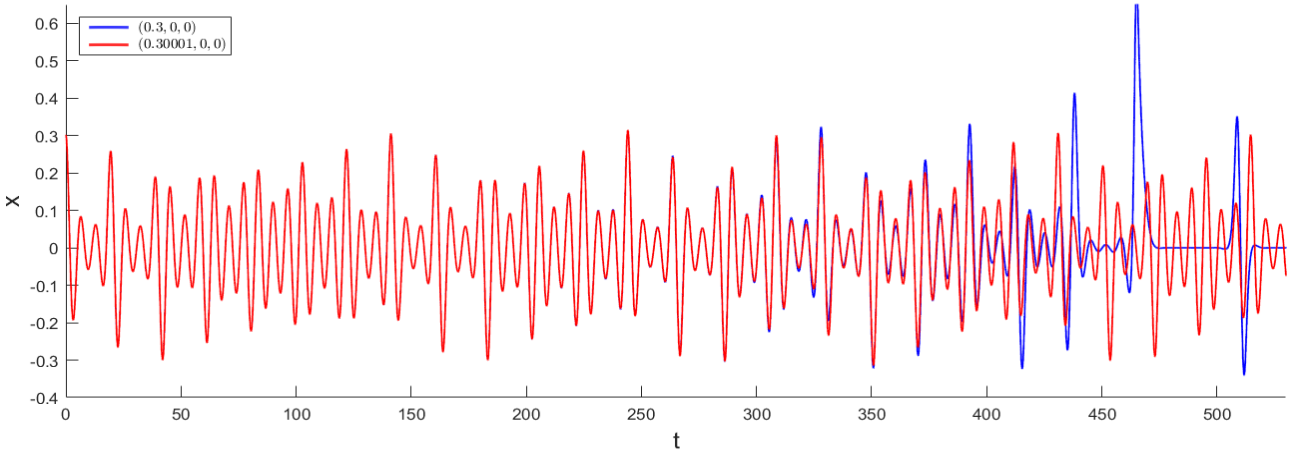

Figure 13: The graph of $x(t)$ for the initial values $(0.3, 0, 0)$ in red, and $(0.30001, 0, 0)$ in blue, for $a = 0.1$. The contrast between the graphs shows the sensitivity of the motion to the initial conditions.

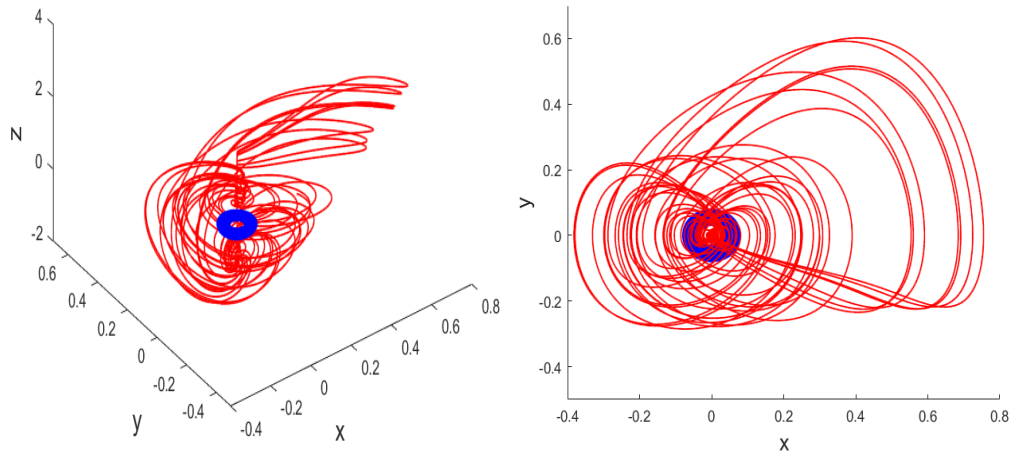

(a) (b)

Figure 14: (a) for $a = 0.01$, the motion of the orbit on a torus with the initial conditions $(0.08, 0, 0)$ in blue and the chaotic attractor with initial conditions $(0.3, 0, 0)$ in red. (b) the projection of the orbits on $xy-$plane.

2.7 The behavior of the orbit in a limit set

The formation of limit set, shown in Figure (10), occurs when a is small and $r_0 > r_a$, where r_a is the initial radius of the periodic orbit corresponding to a, which was found using the averaging method. For the first limit set, $a = 0.0001$, the orbit gets very close to $z-$axis until $\dot{z} = 0$, which corresponds to the first turning point, Figure (15). Afterwards, the orbit oscillates around the z-axis, where $z(t)$ reaches the second turning point, and then increases rapidly so that $z(t)$ reaches the next turning point. This process is repeated showing that the behaviour of $z(t)$, for the corresponding initial values and the value of a, is periodic . However, the Poincare sections in Figure (17) show that the motion of orbit is not periodic but chaotic. In Figure (15b), we see that the behaviour of $z(t)$ during the formation of the limit set, for the same value of a but a different initial point, is the same as Figure (15a), although the first turning points are different. This implies that the amplitude of the motion of the orbit on the $z-$axis and the period of the time between two turning points, during the increase and the decrease of $z(t)$, are the same; the amplitude is approximately 0.2 and the time intervals between two turning points; $T_1 \approx 2000$ time steps when $\dot{z} < 0$ and $T_2 \approx 90$ time steps when $\dot{z} > 0$.

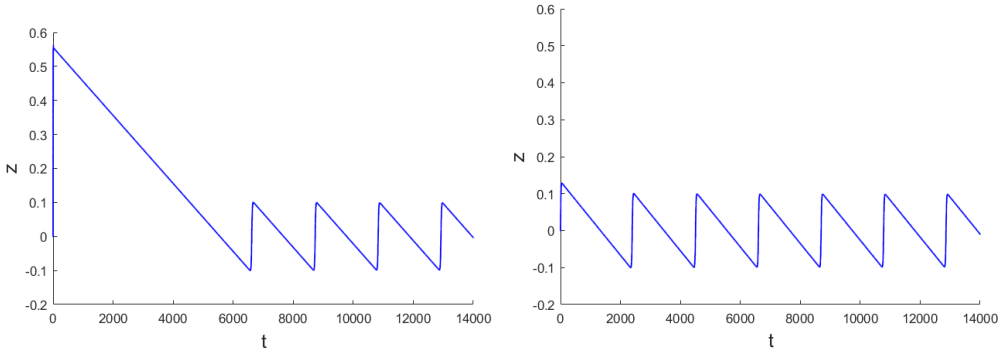

(a) (b)

Figure 15: (a) the projection of the orbit on $z-$axis for $a = 0.0001$ and for the initial point $(0.2, 0, 0)$ and for the initial point $(0.05, 0, 0)$, (b). The same limit set is formed in both cases.

During the formation of the limit set, the increasing rate of $z(t)$ corresponds to the part of the orbit, Figure (10a,b in red), where the radius r increases rapidly for a short period of time, T_2, and then decreases for a period of time T_1.

Moreover, T_2 is shorter than T_1 as shown in the first limit set of the figure where $T_1 \approx 22T_2$. However, the change in r over time explains why the value of $r(t)$ changes in a pulsating manner, Figure $(16b)$.

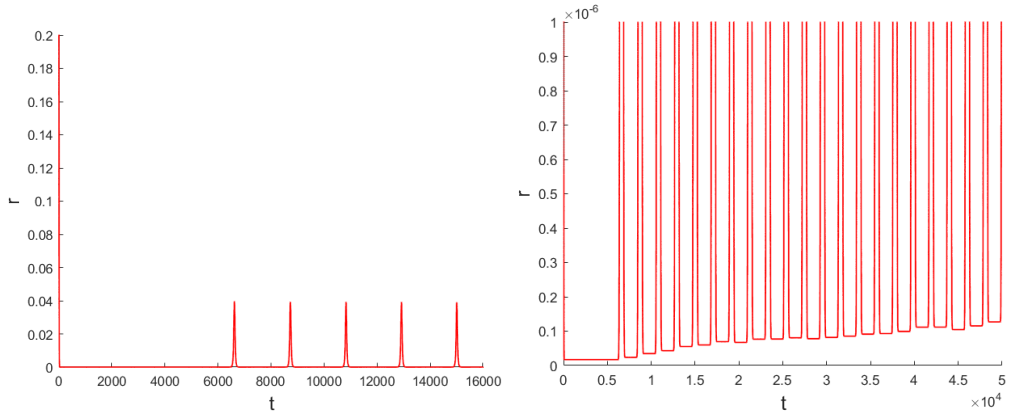

(a) (b)

Figure 16: (a) $r(t)$ behaviour for $a = 0.0001$ and the initial point $(0.2, 0, 0)$. The pulses of r for a short period of time is created when the orbit leaves $z-$axis during the formation of the limit set. (b) the orbit gets very close to $z-$axis in a very short time, and then the r becomes of the order 10^{-7}.

During the formation of the limit set, the orbit gets very close to $z-$axis and spirals down along the axis without intersecting with the axis as shown in section (1,1). Moreover, the radius of the orbit in the neighbourhood of $z-$axis when $\dot{z} < 0$ becomes of the order 10^{-7}, as shown in Figure (16b),and the radius changes at every turn during the spiraling down along $z-$axis. Furthermore, by comparing $r(t)$ with $z(t)$ graphs, we notice that the time interval of the pulses in (t, r) graph corresponds to the time where $\dot{z} > 0$. However, the time intervals where $\dot{z} < 0$ corresponds to the time intervals where $r \approx 0$, during which $r \ll a$, as determined by comparing the value of a and the length of the radius in Figure (16b). Moreover, since $\max|z| \approx 0.1$, Figure (15), the first two terms of $\dot{z}$, equation (2.1), are negligible compared with $a = 0.0001$, therefore the changing rate of $z(t)$ becomes approximately $\dot{z} = -a$ that implies that $z(t)$ can be approximated by the formula:

$$z(t) = z_0 - at, \tag{2.29}$$

and therefore, $T_1 = (z_{\max} - z_{\min}) \times \frac{1}{a} = \frac{l}{a}$, where l is the amplitude of the motion on the z-axis. This equation can be applied to the aforementioned example in Figure (15) which gives $T_1 = \frac{0.2}{0.0001} = 2000$ time steps.

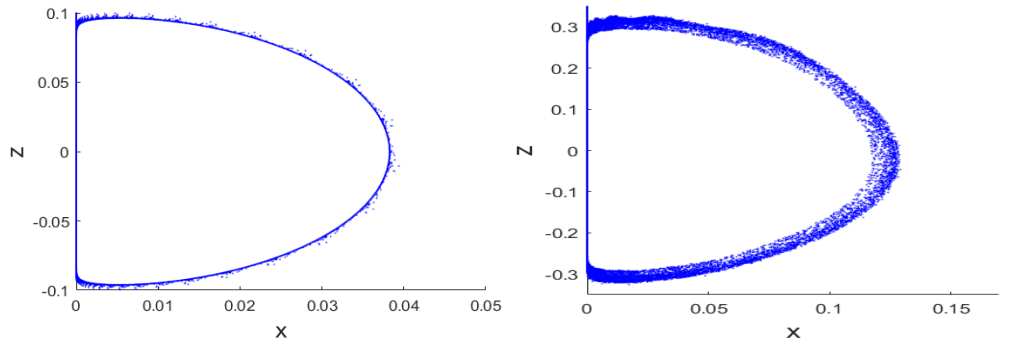

(a) (b)

Figure 17: Poincare sections for the initial values $(0.2, 0, 0)$. (a) $a = 0.0001$ where the chaotic region starts to appear. (b) $a = 0.001$, it shows the increasing of the chaotic region.

Increasing the value of the parameter a to a certain value, at the same initial point, increases the size of the limit set and the chaotic region, Figure (17). However, the behaviour of $z(t)$ and $r(t)$ does not change and the relation $T_1 = \frac{l}{a}$ is still satisfied, Figure (18). This implies that the chaotic behavior starts when a limit set is created and when a increases it eventually evolves to a chaotic attractor as explained in the previous section.

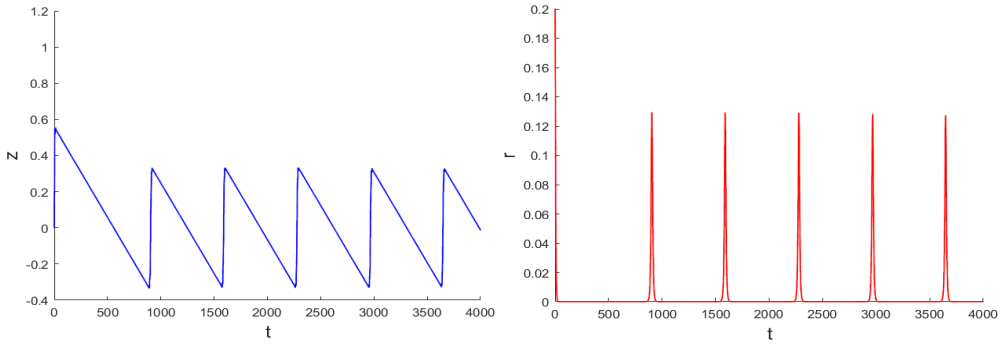

(a) (b)

Figure 18: (a) the behaviour of $z(t)$ for $a = 0.001$ and for the initial values $(0.2, 0, 0)$. (b) $r(t)$ for the same conditions. The graphs show that both variables follows the same behaviour for $a = 0.0001$ while the amplitude on $z-$axis increases as well as the maximum value of $r(t)$.

It can be shown numerically that the behaviour of the orbit is periodic at some initial conditions, such as a is small and r_0 is relatively larger than r_a. For example, the orbit corresponding to the initial conditions $a = 0.001$ and $(0, 0.100042, 0)$ behaves periodically. However, it is numerically difficult to find the exact initial conditions that correspond to a periodic orbit.

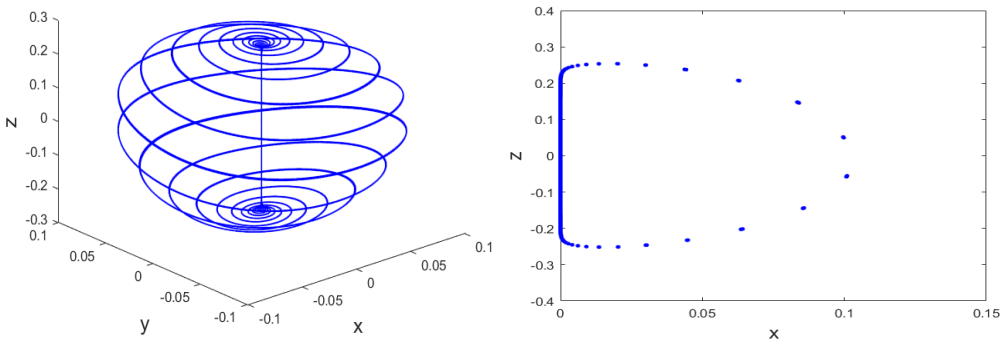

(a) (b)

Figure 19: (a) an orbit corresponding to $a = 0.001$ and to the initial values $(0, 0.100042, 0)$. (b) Poincare sections of the orbit in (a). Both the orbit and the Poincare sections corresponds to 10000 time steps.

Generally, when a is of $O(\varepsilon)$ and the initial radius r_0 is large compared to the initial radius of the periodic solution r_a, the corresponding orbit behaves similarly to the example shown in Figure (19). However, under these aforementioned conditions the orbit does not necessarily behave periodically, but the decreasing rate of z will always be approximately linear and r will always exhibit pulses. Moreover, when the initial radius increases, for a small fixed a, the decreasing rate of z decreases and its increasing rate increases.

In the following, we use Floquet theorem to give the necessary condition for the periodicity of an orbit. Furthermore, we show numerically that this condition is satisfied for the predicted periodic orbit.

Theorem 1 (Floquet).
Consider the system $\dot{x} = A(t)x \ ; \ t \in \mathbb{R}$ where $A(t)$ a continuous $T-$periodic $n \times n-$ matrix. Each fundamental matrix $\Phi(t)$ of the system can be written as the product of $n \times n$ matrices

$$\Phi(t) = P(t)e^{Bt}$$

with $P(t)$ is $T-$periodic and B a constant $n \times n-$matrix.

Remark: The matrix $C = e^{BT}$ is called the monodromy-matrix of the system. The eigenvalues ρ of C are called the characteristic multipliers. Each complex number λ such that

$$\rho = e^{\lambda T}$$

is called a characteristic exponent. We can choose the exponents λ such that they coincide with the eigenvalues of the matrix B.

Theorem 2
Suppose the system $\dot{x} = A(t)x$ has characteristic multipliers ρ_i and exponents λ_i, $i = 1, ..., n$, $\rho_i = e^{\lambda_i T}$. Then we have the following expression for the product of the multiplies and the sum of the exponents

$$\rho_1 \rho_2 ... \rho_n = exp(\int_0^T TrA(t)dt), \tag{2.30}$$

$$\sum_{i=1}^{n} \lambda_i = \frac{1}{T}\int_0^T TrA(t)dt (mod \frac{2\pi i}{T}). \tag{2.31}$$

To apply Floquet theorem, we consider the system

$$\begin{aligned} \dot{x} &= y \\ \dot{y} &= -x - yz \end{aligned} \tag{2.32}$$

which consists of the first two equations of the NE9 system.

Assuming that $z(t)$ is $T-$periodic then from the system (2.32) we find that the matrix of coefficients

$$A(t) = \begin{bmatrix} 0 & 1 \\ -1 & z(t) \end{bmatrix}$$

is also $T-$ periodic. Moreover, if $x(t)$ and $y(t)$ are periodic then from theorem (1) the matrix of coefficients B has two conjugates eigenvalues $\lambda_{1,2} = \pm \omega i$. From the previous remark and theorem (2) we find that

$$\int_0^T z(t)dt = 0. \tag{2.33}$$

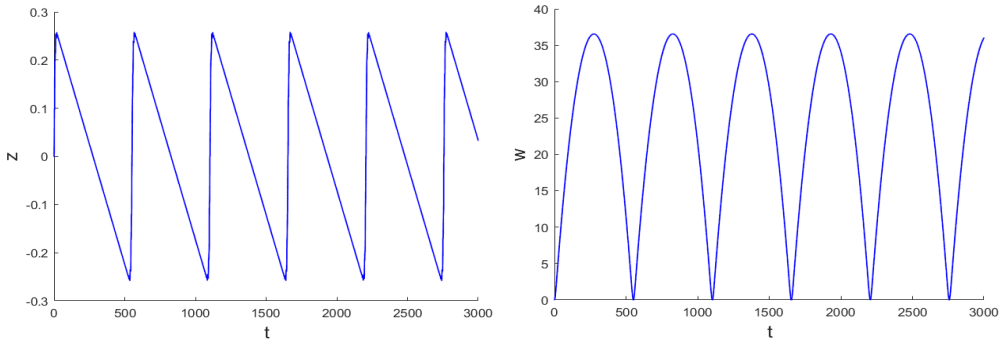

(a) (b)

Figure 20: (a) the behaviour of $z(t)$ for $a = 0.001$ and $(0, 0.100042, 0)$.(b) $w(t) = \int_0^t z(t)dt$ for the same initial conditions, which shows that the necessary condition for the periodic motion is satisfied.

From Figure (20) we notice that the necessary condition (2.33) is satisfied, where $w(t) = \int_0^t z(t)dt$. The figure shows that w is also periodic and the period of the motion is almost 550 time steps

2.8 The limit cycles at different values of the parameter

We have found for a is small, the system, for the corresponding initial point, has a periodic orbit and the motion in its neighbourhood is a quasi-periodic. However, for relatively larger values of a ,in a certain range, the orbit ends at a limit cycle that is changing when a changes. In the following figures we can see that increasing the value of a, within the determined range, either creates a new limit cycle or expand it to a certain size.

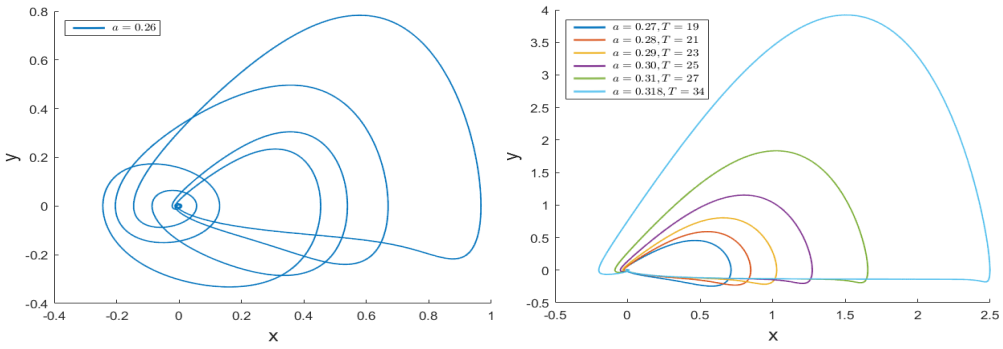

(a) (b)

Figure 21: The projection of the limit cycles on $xy-$plane for a range of the initial values of a, where T represent the period of the limit cycle. We notice that a slight increase to $a = 0.26$ change the formation of the limit cycle, where the new limit cycle expand as a increases in a certain range.

The behavior of the limit cycles shows that the relation between a and T is approximately linear, Figure (21b). Furthermore, this behaviour is repeated for a different range of the values of a, Figure (22b).

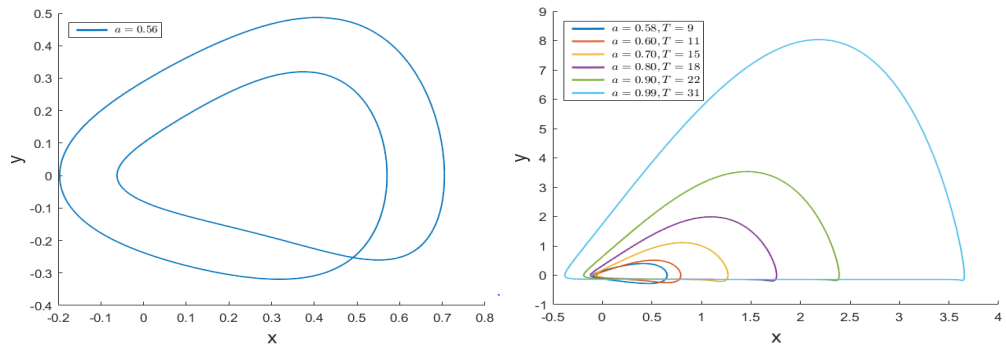

(a) (b)

Figure 22: The projection of the limit cycles on $xy-$plane for a range of the initial values of a. We notice that a slight increase to $a = 0.56$ change the formation of the limit cycle, where the new limit cycle expand as a increases in a certain range.

Furthermore, a cascade of period doublings leads to choas that appears in the system for a small range of a values, as shown in the bifurcation diagram Figure(23a). The appearance of chaos is confirmed by the largest value of the Lyapunov exponents, Figure(23b).

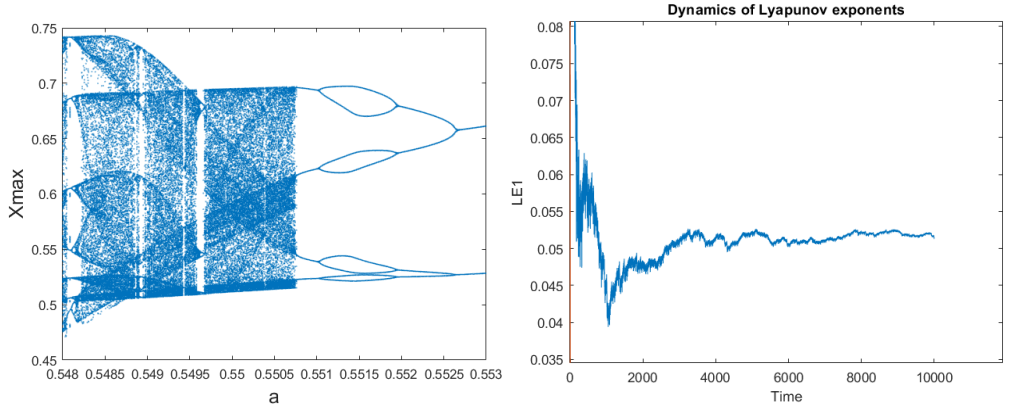

(a) (b)

Figure 23: (a) the bifurcation diagram for $a \in [0.548, 0.553]$ and for the initial point $(0.5, 0, 0)$ of NE9 system. It indicates that the system has a cascade of period doublings that leads to chaos and begins at approximately $a = 0.551$.(b) the change of largest Lyapunov exponent (LE1) over time, for the initial conditions $a = 0.55$ and $(0.5, 0, 0)$. The (LE1) values are positive, which confirms the occurrence of chaos.

2.9 The unbounded behaviour of the orbit and the chaotic attractor

The orbit has an unbounded behaviour when $a \in [0.32, 0.54] \cup [1.1, 1.5]$, which occurs under the following conditions:
• when x becomes negative and bounded by a very small neighbourhood.
• when y, the changing rate of x, becomes very small
• when z becomes very large.
• when the previous conditions lead the changing rate $\dot{y} = -x - yz$ to be very small.
When these conditions are satisfied, the first term of $\dot{z} = -xz + 7x^2 - a$, becomes the dominant one and leads to the rapid increase in $z(t)$. This implies that for those values of the parameter a the motion of the orbit is unbounded from above, Figure (24). Furthermore, since y is very small during the increase of z then x can be considered a fixed value or

bounded in a very small neighbourhood, which implies that the increase of z is exponential. This conclusion is shown for $x = x_0$ as follows:

$$\dot{z} = -x_0 z + 7x_0^2 - a \implies \frac{-x_0\dot{z}}{-x_0 z + 7x_0^2 - a} = -x_0 \text{ and by taking the integral}$$

$$\ln(-x_0 z + 7x_0^2 - a) = -x_0 t + c \implies -x_0 z + 7x_0^2 - a = c_1 e^{-x_0 t} \;;\; c_1 = e^c > 0 \text{ and hence}$$

$$z(t) = \frac{c_1}{-x_0} e^{-x_0 t} + 7x_0 - \frac{a}{x_0} \;;\; x_0 < 0.$$

This implies that $z(t)$ increases exponentially over time and its increasing rate is proportional to the value of x_0. Therefore, the increasing rates of z become higher when a increases within the ranges of a values given in Figure (24).

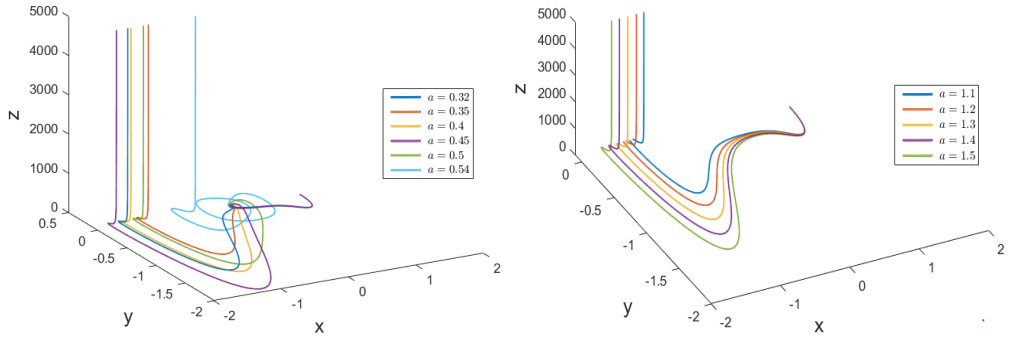

(a) (b)

Figure 24: The unbounded behaviour of the orbit for the values of the parameter a shown and for the initial point $(1,0,0)$.

Remark: The unbounded behaviour of the system occurs for $a \in [0.1, 0.25] \cup [0.32, 0.54] \cup [1.1, 1.5]$, the last two ranges are shown in Figure (24), and for $a > 1.5$.

However, in a small neighbourhood of $a = 0.55$ we notice that the system has a chaotic attractor, which is illustrated by the Poincare sections and the Lyapunov exponents (LE) and Kaplan-Yorke dimension (D_{KY}), Figure (25). The Poincare sections illustrate that the orbit is dense on a three dimensional surface that the orbit lays on. The chaotic behavior is also illustrated by the values $LE_1 = 0.0504, LE_2 \approx 0, LE_3 = -0.3264$ and $D_{KY} = 2.1544$.

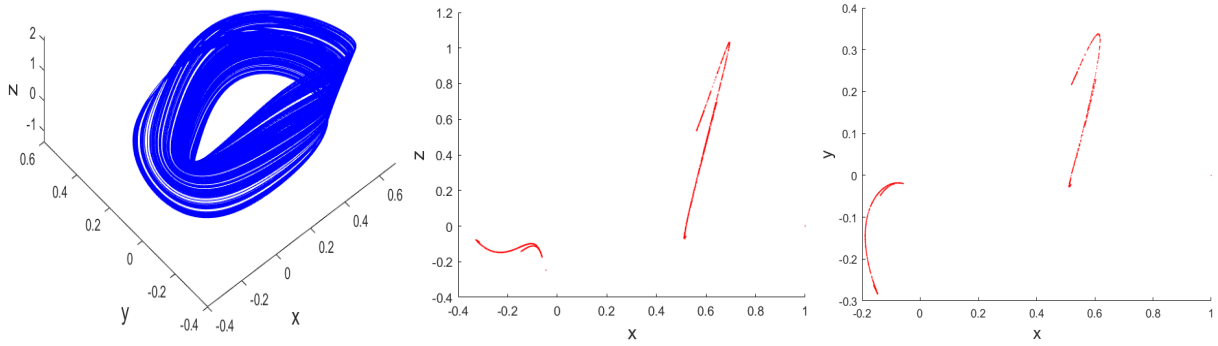

(a) (b) (c)

Figure 25: (a) the chaotic attractor for the initial conditions $a = 0.55$ and $(0.5, 0, 0)$. (b) and (c) the Poincare sections on $xz-$ and $xy-$planes, respectively.

3 NE8 System

The differential system NE8 is :

$$\dot{x} = y, \;\; \dot{y} = -x - yz, \;\; \dot{z} = xy + 0.5x^2 - a. \tag{3.1}$$

In the following we give some properties to the system and we apply averaging method to find an $O(\varepsilon)$ periodic solution of the system in an (ε) neighbourhood of the origin. Moreover, we apply Poincare-Lindstedt method to find a second order analytical approximation to the periodic solution with respect to (ε).

3.1 Some properties of the system

From system (3.1) we find that the system is symmetric with respect to $z-$axis so that for every solution $(x(t), y(t), z(t))$ to the system the orbit $(-x(t), -y(t), z(t))$ is also a solution to the system.

The system in cylindrical coordinates is:

$$\begin{aligned} \dot{r} &= -rz\sin^2\phi, \\ \dot{\phi} &= -1 - \frac{1}{2}z\sin(2\phi), \\ \dot{z} &= \frac{1}{2}r^2\sin(2\phi) + \frac{1}{2}r^2\cos^2\phi - a. \end{aligned} \tag{3.2}$$

The third equation of the system can be written in the form:

$$\dot{z} = \frac{r^2}{4}[\sqrt{5}\cos(2\phi - \alpha) + 1] - a \;\; ; \;\; \alpha \cong 63.43^\circ. \tag{3.3}$$

This implies that $\dot{z} \leq 0$ for one complete turn when $(\frac{\sqrt{5}+1}{4})r^2 - a \leq 0$, which is equivalent to $r \leq \frac{2\sqrt{a}}{\sqrt{\sqrt{5}+1}}$. Therefore, the maximum value of the radius equals to the radius of a circle the is tangent to the hyperbola $xy + \frac{1}{2}x^2 - a = 0$ as it is shown in Figure (26). The value of α represents the angle between the asymptotic lines of the hyperbola branches; $x = 0$ and $y + \frac{1}{2}x = 0$.

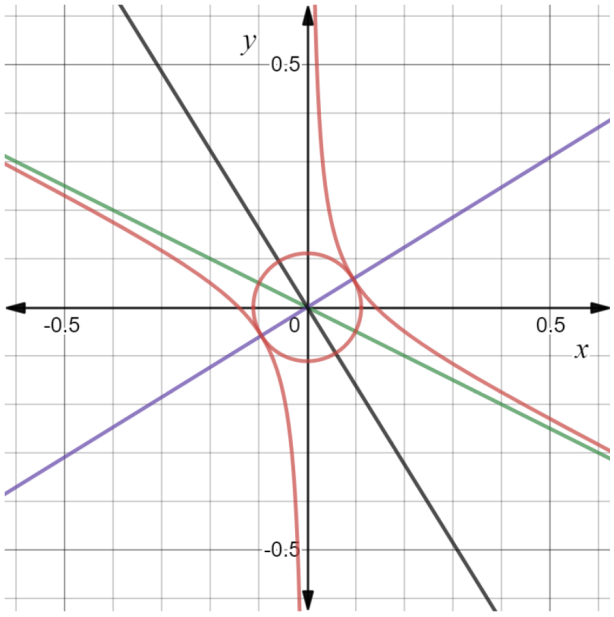

Figure 26: The equation of the hyperbola in red $\dot{z} = 0$ and the equation of the circle is $x^2 + y^2 = \frac{4a}{\sqrt{5}+1}$, where $a = 0.01$.

Furthermore, for $a=0$, every point on the $z-$axis is a critical points of the system, and by following the same procedure of studying the behaviour of the flow in the neighbourhood of the critical points we find that the eigenvalues of the critical point $(0,0,z_0)$ are

$$\lambda_1 = \frac{-z_0}{2} - \sqrt{\frac{z_0^2}{4}-1} = \frac{-z_0}{2} - \frac{1}{2}\sqrt{z_0^2-4},$$
$$\lambda_2 = \frac{-z_0}{2} + \sqrt{\frac{z_0^2}{4}-1} = \frac{-z_0}{2} + \frac{1}{2}\sqrt{z_0^2-4},$$
$$\lambda_3 = 0,$$

which are identical to the eigenvalues of the NE9 system at the same critical point. This implies that the behaviour of the flow of the NE8 system and NE9 system in the neighbourhood of the critical point is similar. Furthermore, the corresponding eigenvectors are

$$v_1 = (1, -\frac{1}{2}(z_0+\sqrt{z_0^2-4}), 0) \ , \ v_2 = (1, \frac{1}{2}(z_0+\sqrt{z_0^2-4}), 0) \ , \ v_3 = (0,0,1).$$

For $-2 < z_0 < 2$, we get two conjugate complex eigenvalues ,and moreover a complex component in v_1 and v_2, which indicates the spiral behaviour of the flow in the neighbourhood of the critical point in this case.

3.2 The first and the second order calculation using averaging method

In this section, we apply the same calculation methods of averaging we applied on the NE9 system. Furthermore, we compare between the results of the first and the second order averaging.

3.2.1 First order averaging

The first two equations in system (3.1) are reduced to one differential equation as the following:

$$\ddot{x} = \dot{y} = -x - yz \implies \ddot{x} + x = -\dot{x}z. \tag{3.4}$$

Then we make the following rescaling of the variables around the origin

$$x = \varepsilon\bar{x}, \ \ y = \varepsilon\bar{y}, \ \ z = \varepsilon\bar{z}, \ \ a = \varepsilon^2 a_0.$$

Here we scaled the parameter a around zero of order (ε^2) for consistency. Moreover, the scaling of x and y implies that $r = \varepsilon\bar{r}$; $\bar{r} = \sqrt{\bar{x}^2+\bar{y}^2}$.

Substituting in (3.4) and in the expression of $\dot{z}$ of system (3.1). After leaving out the bars we get the following two equations:

$$\begin{aligned} \ddot{x} + x &= -\varepsilon\dot{x}z, \\ \dot{z} &= \varepsilon(xy + 0.5x^2 - a_0). \end{aligned} \tag{3.5}$$

For $\varepsilon \neq 0$ we assume that the first equation of system (3.5) has the solution

$$x = r\cos(t+\psi), \ \ \dot{x} = -r\sin(t+\psi). \tag{3.6}$$

Substitution of these expressions for x and $\dot{x}$ into the first equation of system (3.5) yields

$$-\dot{r}\sin(t+\psi) - r\cos(t+\psi)\dot{\psi} = -\varepsilon\dot{x}z. \tag{3.7}$$

From the form of the solution (3.6) we find that

$$\frac{d}{dt}[r\cos(t+\psi)] = -r\sin(t+\psi),$$

which gives the following differential equation

$$\dot{r}\cos(t+\psi) - \dot{\psi}r\sin(t+\psi) = 0, \tag{3.8}$$

We consider (3.7) and (3.8) as two algebraic equations in $\dot{r}$ and $\dot{\psi}$, therefore the solution of the two equations is

$$\dot{r} = -\varepsilon r z \sin^2(t+\psi), \;\; \dot{\psi} = -\frac{1}{2}\varepsilon z \sin(2t+2\psi). \tag{3.9}$$

Averaging over z in system (3.5) gives

$$\begin{aligned}
\dot{z}_A &= \frac{1}{2\pi}\int_0^{2\pi} \varepsilon[r_A^2\cos(t+\psi_A)\sin(t+\psi_A) + r_A^2\cos^2(t+\psi_A) - a_0]dt \\
&= \frac{1}{2\pi}\int_0^{2\pi} \varepsilon(r_A^2\frac{1+\cos(2t+2\psi_A)}{4} - a_0)dt \\
&= \varepsilon(\frac{r_A^2}{4} - a_0).
\end{aligned}$$

and averaging over r and ψ in system (3.9) gives

$$\begin{aligned}
\dot{r}_A &= \frac{1}{2\pi}\int_0^{2\pi} -\varepsilon r_A z_A \frac{1-\cos(2t+2\psi_A)}{2}dt = \frac{-\varepsilon r_A z_A}{2}, \\
\dot{\psi}_A &= \frac{1}{2\pi}\int_0^{2\pi} -\varepsilon z_A \frac{\sin(2t+2\psi_A)}{2}dt = 0 \implies \psi_A = \psi_0.
\end{aligned}$$

So the averaging method produces the following system of ODEs:

$$\begin{aligned}
\dot{r}_A &= \frac{-1}{2}\varepsilon r_A z_A, \\
\dot{\psi}_A &= 0, \\
\dot{z}_A &= \varepsilon(\frac{r_A^2}{4} - a_0).
\end{aligned} \tag{3.10}$$

It is clear that $(2\sqrt{a_0}, \psi_A, 0)$ is a critical point of the system. To find initial values of a periodic solution we start ,for example, with the following values $a_0 = 1 \implies r_A = 2$, and $\varepsilon = 10^{-3} \implies a = 10^{-6}$. In system (3.1) we know that $r = \varepsilon\bar{r} = \varepsilon r_A = 0.002$ and since $r = \sqrt{x^2+y^2}$ then $r = x = 0.002$ when $y = 0$. Therefore, for $\psi_A = 0$ the point $(0.002, 0, 0)$ is an initial value corresponds to a periodic solution to the system (3.1) for $a = 10^{-6}$, Figure (27).

The characteristic equation of the Jacobian of system (3.10) at the critical point is

$$\lambda(\lambda^2 + \frac{1}{4}\varepsilon^2 r_A^2) = 0.$$

Therefore, the eigenvalues at that point are $\lambda_1 = 0$, $\lambda_{2,3} = \pm\frac{1}{2}\varepsilon i r_A$ which implies that there exists an isolated 2π periodic solution in an $O(\varepsilon)$ neighbourhood of the origin as it is shown in Figure (27) and it is ,at this level of approximation, L-stable.

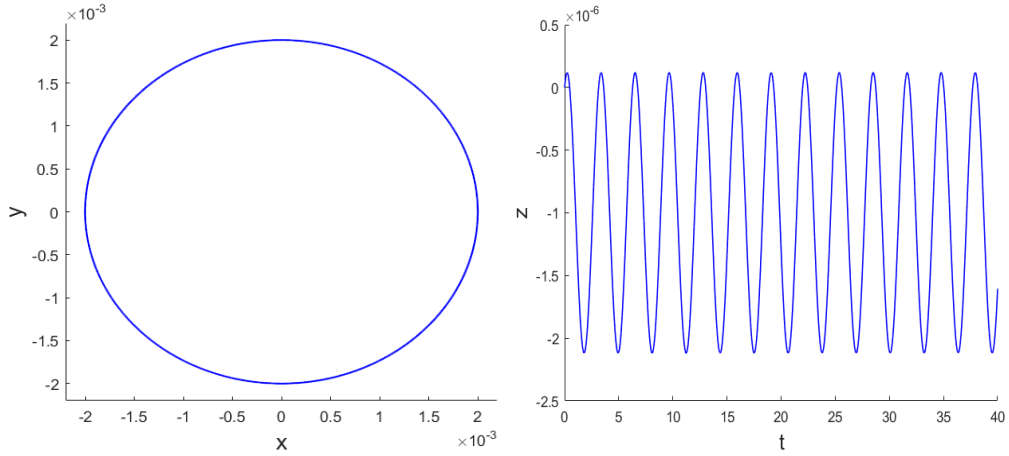

(a) (b)

Figure 27: (a) the periodic solution in (x,y,z) coordinate system. (b) the periodic motion on $z-$axis. Both of them correspond to the initial values $(0.002,0,0)$, $a = 10^{-6}$ and $\varepsilon = 10^{-3}$.

Remark: From the third equation in system (3.10) we conclude that z_a is always increasing in a neighbourhood of (ε) when $a = a_0 = 0$.

From the averaged system (3.10) we show,using separation of variables, that the system has a first integral

$$\frac{dr_A}{dz_A} = \frac{-r_A z_A}{\frac{r_A^2}{2} - 2A_0}$$
$$\frac{r_A^2 - 4a_0}{2r_A} dr_A = -z_A dz_A$$
$$(\frac{r_A}{2} - \frac{2A_0}{r_A}) dr_A = -z_A dz_A$$
$$\frac{r_A^2}{4} - 2A_0 \ln r_A = -\frac{1}{2} z_A^2 + c \ ; \ c \in \mathbb{R}.$$

Therefore, the algebraic equations

$$r_A^2 - 8a_0 \ln r_A + 2z_A^2 = c_1$$
$$\psi_A = \psi_0 \quad ; \quad c_1 \ , \ \psi_0 \in \mathbb{R},$$

represent a first integral of the averaged system (3.10), where the constants c_1 and ψ_0 are determined uniquely for some initial values and a value of a_0

3.2.2 The second order averaging

The differential system NE8 is:

$$\dot{x} = y \ , \ \dot{y} = -x - yz \ , \ \dot{z} = xy + 0.5x^2 - a. \tag{3.11}$$

After applying the following rescaling around the origin

$$x = \varepsilon \bar{x}, \ y = \varepsilon \bar{y}, \ z = \varepsilon \bar{z}, \ a = \varepsilon^2 a_0 \ ; \ a_0 = O(1).$$

we get, after leaving out the bars, the following differential equations

$$\dot{x} = y \ , \ \dot{y} = -x - \varepsilon yz \ , \ \dot{z} = \varepsilon(xy + 0.5x^2 - a_0). \tag{3.12}$$

Introducing amplitude phase-variables $x(t) = r(t)\cos(t+\psi(t))$, $\dot{x}(t) = -r(t)\sin(t+\psi(t))$ and by doing similar steps to what we do in the first order averaging to get the algebraic system (3.7) and (3.8) we get the following system:

$$\begin{aligned} \dot{r} &= -\varepsilon rz\sin^2(t+\psi), \\ \dot{\psi} &= -\frac{1}{2}\varepsilon z\sin(2t+2\psi), \\ \dot{z} &= \varepsilon(-\frac{1}{2}r^2\sin(2t+2\psi) + \frac{1}{2}r^2\cos^2(t+\psi) - a_0). \end{aligned} \tag{3.13}$$

System (3.13) has the form $\dot{V} = \varepsilon f(t,V)$ where $V = (r,\psi,z)$ and

$$f(t,r,\psi,z) = \begin{bmatrix} -\frac{rz}{2} + \frac{rz}{2}\cos 2\alpha \\ -\frac{z}{2}\sin 2\alpha \\ -\frac{1}{2}r^2\sin 2\alpha + \frac{1}{4}r^2\cos 2\alpha + \frac{1}{4}r^2 - a_0 \end{bmatrix} \implies f^0(r,\psi,z) = \begin{bmatrix} -\frac{rz}{2} \\ 0 \\ \frac{r^2}{4} - a_0 \end{bmatrix}, \tag{3.14}$$

where $\alpha = t + \psi$. The gradient of f is:

$$\nabla f = \begin{bmatrix} -\frac{z}{2} + \frac{z}{2}\cos 2\alpha & -rz\sin 2\alpha & -\frac{r}{2} + \frac{r}{2}\cos 2\alpha \\ 0 & -z\cos 2\alpha & -\frac{1}{2}\sin 2\alpha \\ -r\sin 2\alpha + \frac{1}{2}r\cos 2\alpha + \frac{r}{2} & -r^2\cos 2\alpha - \frac{r^2}{2}\sin 2\alpha & 0 \end{bmatrix}. \tag{3.15}$$

We have the vector field $u^1(t,x) = \int_0^t (f(s,x) - f^0(x))ds - a(x)$; $a(x)$ chosen such that the average of u^1 vanishes. Therefore we have:

$$u^1 = \begin{bmatrix} \frac{rz}{4}\sin 2\alpha \\ \frac{z}{4}\cos 2\alpha \\ \frac{r^2}{4}\cos 2\alpha + \frac{1}{8}r^2\sin 2\alpha \end{bmatrix}. \tag{3.16}$$

We have to calculate $f^1 = \nabla f u^1$

$$f^1 = \begin{bmatrix} -\frac{z}{2} + \frac{z}{2}\cos 2\alpha & -rz\sin 2\alpha & -\frac{r}{2} + \frac{r}{2}\cos 2\alpha \\ 0 & -z\cos 2\alpha & -\frac{1}{2}\sin 2\alpha \\ -r\sin 2\alpha + \frac{1}{2}r\cos 2\alpha + \frac{r}{2} & -r^2\cos 2\alpha - \frac{r^2}{2}\sin 2\alpha & 0 \end{bmatrix} \begin{bmatrix} \frac{rz}{4}\sin 2\alpha \\ \frac{z}{4}\cos 2\alpha \\ \frac{r^2}{4}\cos 2\alpha + \frac{1}{8}r^2\sin 2\alpha \end{bmatrix} \tag{3.17}$$

$$= \begin{bmatrix} (-\frac{z}{2} + \frac{z}{2}\cos 2\alpha)(\frac{rz}{4}\sin 2\alpha) + (-rz\sin 2\alpha)(\frac{z}{4}\cos 2\alpha) + (-\frac{r}{2} + \frac{r}{2}\cos 2\alpha)(\frac{r^2}{4}\cos 2\alpha + \frac{1}{8}r^2\sin 2\alpha) \\ (-z\cos 2\alpha)(\frac{z}{4}\cos 2\alpha) + (-\frac{1}{2}\sin 2\alpha)(\frac{r^2}{4}\cos 2\alpha + \frac{1}{8}r^2\sin 2\alpha) \\ (-r\sin 2\alpha + \frac{1}{2}r\cos 2\alpha + \frac{r}{2})(\frac{rz}{4}\sin 2\alpha) + (-r^2\cos 2\alpha - \frac{r^2}{2}\sin 2\alpha)(\frac{z}{4}\cos 2\alpha) \end{bmatrix}.$$

and after averaging we get:

$$f_1^0(r,\psi,z) = \begin{bmatrix} \frac{r^3}{16} \\ -\frac{z^2}{8} - \frac{r^2}{32} \\ \frac{-r^2z}{4} \end{bmatrix}. \tag{3.18}$$

Therefore, we get a an $O(\varepsilon^2)$ system of the form

$$\dot{V} = \varepsilon f^0(V) + \varepsilon^2 f_1^0(V), \tag{3.19}$$

which can be written as

$$\dot{r}_a = \frac{-\varepsilon r z}{2} + \frac{\varepsilon^2 r^3}{16},$$
$$\dot{\psi}_a = -\varepsilon^2(\frac{z^2}{8} + \frac{r^2}{32}),$$
$$\dot{z}_a = \varepsilon(\frac{r^2}{4} - a_0) - \varepsilon^2(\frac{r^2 z}{4}).$$

We notice that $(2\sqrt{a_0}, \psi_0, \frac{\varepsilon a_0}{2})$ is a fixed point to the system of $O(\varepsilon^2)$. In the following we calculate the Jaconbian of the last system and calculate the eigenvalues at the critical point.

$$J = \begin{bmatrix} \frac{-\varepsilon z}{2} + \frac{3\varepsilon^2 r^2}{16} & 0 & \frac{-\varepsilon r}{2} \\ -\frac{\varepsilon^2 r}{16} & 0 & -\frac{\varepsilon^2 z}{4} \\ \frac{\varepsilon r}{2} - \frac{\varepsilon^2 r z}{2} & 0 & -\frac{\varepsilon^2 r^2}{4} \end{bmatrix} \Longrightarrow J|_{(2\sqrt{a_0}, \psi_0, \frac{\varepsilon a_0}{2})} = \begin{bmatrix} \frac{\varepsilon^2 a_0}{2} & 0 & -\varepsilon\sqrt{a_0} \\ -\frac{\varepsilon^2\sqrt{a_0}}{8} & 0 & -\frac{\varepsilon^2 a_0}{8} \\ \varepsilon\sqrt{a_0} - \frac{\varepsilon^3 a_0\sqrt{a_0}}{2} & 0 & -\varepsilon^2 a_0 \end{bmatrix}, \tag{3.20}$$

and therefore the characteristic equation is:

$$-\lambda[(\lambda - \frac{\varepsilon^2 a_0}{2})(\lambda + \varepsilon^2 a_0) + \varepsilon\sqrt{a_0}(\varepsilon\sqrt{a_0} - \frac{\varepsilon^3 a_0\sqrt{a_0}}{2})] = 0 \tag{3.21}$$
$$\Longrightarrow \lambda(\lambda^2 + \frac{1}{2}\varepsilon^2 a_0\lambda + \varepsilon^2 a_0 - \varepsilon^4 a_0^2) = 0. \tag{3.22}$$

which implies that $\lambda_1 = 0$ and for the quadratic term between brackets we have

$$\Delta = \frac{17\varepsilon^4 a_0^2}{4} - 4\varepsilon^2 a_0 < 0 \Longrightarrow \lambda_{2,3} = -\frac{1}{4}a \pm iO(\varepsilon). \tag{3.23}$$

This implies that the periodic orbit is an attractor and the attracting rate is proportional to the value of a, which is indicated in the Poincare sections in Figure (28). In the same figure (a), we can see that the orbit is approaching the attractor for $a = 10^{-4}$ in 2×10^5 time steps, while for $a = 10^{-6}$ it takes a longer period of time to approach the attractor, which is, based on the figure (b), more that 10^6 time step. Furthermore, since the attracting rate is constant, starting from the initial point $(0.08, 0, 0)$ makes the deviation toward the attractor smaller at every turn. This is because the further the initial point, the longer the time it takes for every turn to be completed. This explains why the intensity of Poincare sections increases when the orbit gets close to the attractor.

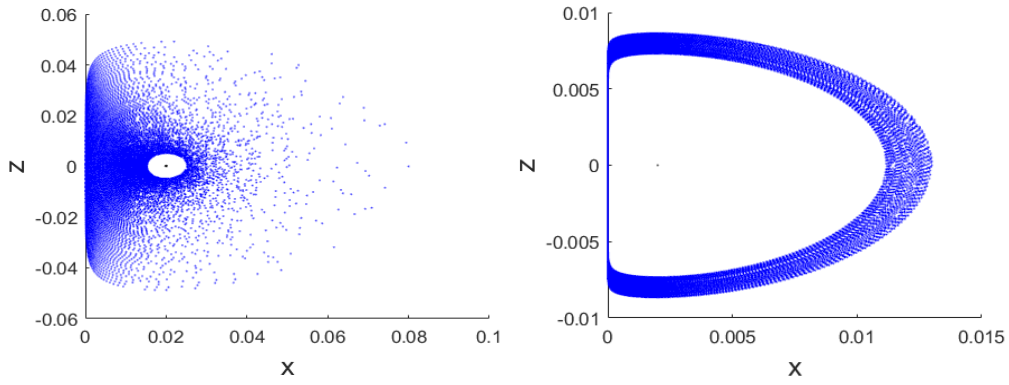

(a) (b)

Figure 28: (b) Poincare sections for $t = 10^6$ time step, $a = 10^{-6}$, and the initial points $(0.002, 0, 0)$ and $(0.013, 0, 0)$, where the first point corresponds to the periodic solution.(a) the Poincare sections for $t = 10^5$ time step, $a = 10^{-4}$, and the initial points $(0.02, 0, 0)$ and $(0.08, 0, 0)$, where the first point correspond to the periodic solution. We notice that as a increases, the converging rate toward the periodic solution also increases.

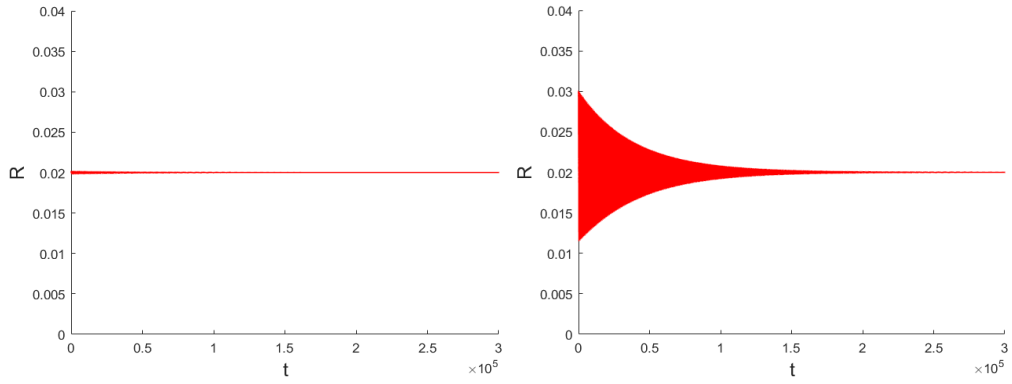

(a) (b)

Figure 29: (a) the behaviour of $R = \sqrt{x^2+y^2+z^2}$ that corresponds to the periodic solution for the initial point $(0.02,0,0)$ and $a = 10^{-4}$. (b) we see how R, starting from the initial value $(0.03,0,0)$, oscillates around the value $R = 0.02$, which corresponds to the periodic solution until it reaches it.

3.3 The second order approximation of the periodic solution using The Poincare-Lindstedt method

In this section, we apply the same calculation method we applied on the NE9 system to find an analytical representation to the periodic orbit of the second order.

The equations we get after re-scaling the variables and the parameter, similar to the process of getting the system of equation (3.5), are:

$$\begin{aligned} \ddot{x}+x &= -\varepsilon \dot{x} z, \\ \dot{z} &= \varepsilon(xy+0.5x^2-\bar{a}). \end{aligned} \tag{3.24}$$

The first equation of system (3.24) has the form:

$$\ddot{x}+x = \varepsilon f(x,\dot{x},z,\varepsilon) \;\; ; \;\; f(x,\dot{x},z,\varepsilon) = -\dot{x}z. \tag{3.25}$$

We make the transformation:

$$\omega t = \theta \;\; ; \;\; \omega^{-2} = 1-\varepsilon\eta(\varepsilon) \implies \frac{1}{\omega} = \sqrt{1-\varepsilon\eta(\varepsilon)}.$$

The first and the second derivative with respect to θ are calculated as the following:

$$\theta = \omega t \implies \frac{d}{dt} = \frac{d\theta}{dt}\frac{d}{d\theta} = \omega\frac{d}{d\theta} \;\text{ and }\; \frac{d^2}{dt^2} = \omega^2\frac{d^2}{d\theta^2}.$$

Using the transforming and the notation $x' = \frac{dx}{d\theta}$, equation (3.25) becomes:

$$x'' + x = \varepsilon[\eta x + (1-\varepsilon\eta) f(x,(1-\varepsilon\eta)^{\frac{-1}{2}}x', z, \varepsilon)], \tag{3.26}$$

$$\text{with initial values } x(0) = a(\varepsilon), x'(0) = 0.$$

By substituting in the last form we get:

$$x'' + x = \varepsilon[\eta x - (1-\varepsilon\eta)^{\frac{1}{2}}x'z]. \tag{3.27}$$

The corresponding periodic solution of equation (3.27) can be represented by the convergent series:

$$x(\theta) = a(0)\cos\theta + \sum_{n=1}^{\infty} \varepsilon^n \gamma_n(\theta) \ \ , \ \ z(\theta) = z_0 + \sum_{n=1}^{\infty} \varepsilon^n z_n(\theta) \ \ ; \ \ z_0 = \text{constant}.$$

in which $\theta = \omega t = (1-\varepsilon\eta)^{\frac{-1}{2}} t$ while using the convergent series:

$$a = \sum_{n=0}^{\infty} \varepsilon^n a_n \ \ , \ \ \eta = \sum_{n=0}^{\infty} \varepsilon^n \eta_n \ \ , \ \ x(0) = a(0) + \sum_{n=1}^{\infty} \varepsilon^n \gamma_n(0) \ \ , \ \ 0 < \varepsilon \leq \varepsilon_0.$$

We have $\frac{1}{\omega} = \sqrt{1-\varepsilon\eta(\varepsilon)}$ and by using Taylor expansion of the function $\frac{1}{\omega}$ around $\varepsilon = 0$ we get:

$$\frac{1}{\omega} = 1 - \frac{1}{2}\varepsilon\eta_0 - \varepsilon^2(\frac{1}{2}\eta_1 + \frac{1}{8}\eta_0^2) + O(\varepsilon^3).$$

To determine $a(0)$ and $\eta(0)$ we substitute in the following equations:

$$\begin{aligned} \int_0^{2\pi} \sin\theta f(a(0)\cos\theta, -a(0)\sin\theta, z_0, 0) d\theta = 0, \\ \pi\eta(0)a(0) + \int_0^{2\pi} \cos\theta f(a(0)\cos\theta, -a(0)\sin\theta, z_0, 0) d\theta = 0. \end{aligned} \tag{3.28}$$

From equation (3.25) we find that:

$$f(a(0)\cos\theta, -a(0)\sin\theta, z_0, 0) = a(0) z_0 \sin\theta.$$

After substituting in system (3.28) we get

$$\begin{aligned} \int_0^{2\pi} \sin\theta (a(0) z_0 \sin\theta) d\theta = 0 \implies -\pi a(0) z_0 = 0, \\ \pi\eta(0)a(0) + \int_0^{2\pi} \cos\theta (a(0) z_0 \sin\theta) d\theta = 0 \implies \pi\eta(0)a(0) = 0. \end{aligned} \tag{3.29}$$

From the second equation of system (3.24) we find that:

$$\omega z' = \varepsilon(xy + 0.5x^2 - \bar{a}) \implies z(\theta) = \frac{1}{\omega}[z(0) + \int_0^{\theta} \varepsilon(xy + 0.5x^2 - \bar{a}) ds].$$

By using the expansion form of the variables we get:

$$\begin{aligned} z(\theta) &= \frac{1}{\omega}[z(0) + \varepsilon \int_0^{\theta} (-a_0^2 \cos s \sin s + 0.5 a_0^2 \cos^2 s - \bar{a} + O(\varepsilon)) ds] \\ &= \frac{1}{\omega}[z(0) + \varepsilon \int_0^{\theta} (-a_0^2 \cos s \sin s + \frac{a_0^2}{4}(1 + \cos 2s) - \bar{a} + O(\varepsilon)) ds]. \end{aligned}$$

If z is periodic then z is bounded, which requires cancelling the secular terms in the last formula of z which implies that:

$$\frac{a_0^2}{4} - \bar{a} = 0 \implies a_0 = 2\sqrt{\bar{a}}. \tag{3.30}$$

Therefore, for $\bar{a} \neq 0$ we get $a_0 = a(0) \neq 0$ and from equations (3.29) we conclude that $z_0 = \eta(0) = 0$. Moreover, from equations (3.29) and equation (3.30) we get the system in a neighbourhood of $\varepsilon = 0$

$$\begin{aligned} F_1(a(0), \eta(0), z_0) &= \frac{a(0)^2}{4} - \bar{a} = 0, \\ F_2(a(0), \eta(0), z_0) &= \pi\eta(0)a(0) = 0, \\ F_3(a(0), \eta(0), z_0) &= -\pi a(0) z_0 = 0, \end{aligned}$$

which implies that

$$\left|\frac{\partial(F_1, F_2, F_3)}{\partial(a(0), \eta(0), z_0)}\right| = \begin{vmatrix} \frac{a(0)}{2} & 0 & 0 \\ \pi\eta(0) & \pi a(0) & 0 \\ -\pi z_0 & 0 & -\pi a(0) \end{vmatrix} = -0.5\pi^2 a(0)^3 \neq 0,$$

therefore we conclude that there is an isolated periodic solution which branches off for $\varepsilon > 0$, that is the same result we got when applying the averaging theorem. Therefore, the periodic solution of (3.27) can be represented by the given convergent series

and from the expansion form of η we get that $\eta_0 = 0$. Therefore, $\frac{1}{\omega}$ has the form:

$$\frac{1}{\omega} = 1 - \frac{1}{2}\varepsilon^2\eta_1 + O(\varepsilon^3).$$

From the expansion form of $x(\theta)$ we find:

$$\begin{aligned} x(\theta) &= a(0)\cos\theta + \varepsilon\gamma_1(\theta) + \varepsilon^2\gamma_2(\theta) + ..., \\ x'(\theta) &= -a(0)\sin\theta + \varepsilon\gamma_1'(\theta) + \varepsilon^2\gamma_2'(\theta) + ..., \\ x''(\theta) &= -a(0)\cos\theta + \varepsilon\gamma_1''(\theta) + \varepsilon^2\gamma_2''(\theta) + ... \end{aligned}$$

By substituting in (3.27), knowing that $z_0 = \eta_0 = 0$, we get:

$$\begin{aligned} \varepsilon(\gamma_1'' + \gamma_1) + \varepsilon^2(\gamma_2'' + \gamma_2) + O(\varepsilon^3) = \varepsilon[(\varepsilon\eta_1 + \varepsilon^2\eta_2^2 + O(\varepsilon^3))(a_0\cos\theta + \varepsilon\gamma_1 + \varepsilon^2\gamma_2 + O(\varepsilon^3)) - (1 - \frac{1}{2}\varepsilon^2\eta_1 + O(\varepsilon^3)) \\ \times (\varepsilon z_1 + \varepsilon^2 z_2 + O(\varepsilon^3))(-a_0\sin\theta + \varepsilon\gamma_1' + \varepsilon^2\gamma_2' + O(\varepsilon^3))]. \end{aligned}$$

By equating with respect to (ε^1) we get:

$$\gamma_1'' + \gamma_1 = 0,$$

which has a general solution of the form:

$$\gamma_1(\theta) = A_1\cos\theta + B_1\sin\theta.$$

Since $x'(0) = 0$ we get $\gamma_1'(0) = 0$. By substituting in the general solution we get $B_1 = 0$. From the initial conditions we have $A_1 = a_1$, and therefore $\gamma_1(\theta) = a_1\cos\theta$

By equating with respect to (ε^2) we get:

$$\gamma_2'' + \gamma_2 = \eta_1 a_0\cos\theta + z_1 a_0\sin\theta. \tag{3.31}$$

To determine z_1 we apply the changing of the variables to the second equation of system (3.24), so we get the equation:

$$\omega z' = \varepsilon(xy + 0.5x^2 - \bar{a}) \implies z' = \frac{\varepsilon}{\omega}(xy + 0.5x^2 - \bar{a}).$$

After writing the last equation in the expansion form knowing that $\eta_0 = z_0 = 0$ we get:

$$\begin{aligned}\varepsilon z_1' + \varepsilon^2 z_2' + O(\varepsilon^3) = \varepsilon(1 - \frac{1}{2}\varepsilon^2\eta_1 + O(\varepsilon^3))[(a_0\cos\theta + \varepsilon\gamma_1(\theta) + \varepsilon^2\gamma_2(\theta) + O(\varepsilon^3))(-a_0\sin\theta + \varepsilon\gamma_1'(\theta) \\ + \varepsilon^2\gamma_2'(\theta) + O(\varepsilon^3)) + 0.5(a_0\cos\theta + \varepsilon\gamma_1(\theta) + \varepsilon^2\gamma_2(\theta) + O(\varepsilon^3))^2 - \bar{a}].\end{aligned} \tag{3.32}$$

By equating both sides of $O(\varepsilon)$ we get:

$$\begin{aligned}z_1'(\theta) &= (-a_0^2\cos\theta\sin\theta + 0.5a_0^2\cos^2\theta - \bar{a}) = \frac{-a_0^2}{2}\sin 2\theta + \frac{1}{4}a_0^2(1+\cos 2\theta) - \bar{a} \implies \\ z_1(\theta) &= z_1(0) + \int_0^\theta [\frac{1}{4}a_0^2 - \bar{a} + a_0^2(\frac{-1}{2}\sin 2s + \frac{1}{4}\cos(2s))]ds\end{aligned}$$

We have $\frac{1}{4}a_0^2 - \bar{a} = 0$ and therefor we get:

$$z_1(\theta) = z_1(0) + a_0^2(\frac{1}{4}\cos(2\theta) + \frac{1}{8}\sin(2\theta) - \frac{1}{4}).$$

By substituting in (3.31) we get:

$$\begin{aligned}\gamma_2'' + \gamma_2 &= \eta_1 a_0\cos\theta + a_0\sin\theta(\frac{a^2}{4}\cos(2\theta) + \frac{a_0^2}{8}\sin(2\theta) + z(0) - \frac{a_0^2}{4}) \\ &= \eta_1 a_0\cos\theta + \frac{a_0^3}{8}(\sin(3\theta) - \sin(\theta)) + \frac{a_0^3}{16}(\cos(\theta) - \cos(3\theta)) + a_0(z(0) - \frac{a_0^2}{4})\sin\theta \\ &= (\eta_1 a_0 + \frac{a_0^3}{16})\cos\theta + (\frac{-3a_0^3}{8} + a_0 z(0))\sin\theta + \frac{a_0^3}{8}\sin 3\theta - \frac{a_0^3}{16}\cos 3\theta.\end{aligned}$$

By applying periodicity conditions we get $\eta_1 = -\frac{a_0^2}{16}$ and $z(0) = \frac{3a_0^2}{8}$. Therefore, the general solution of the equation has the form:

$$\gamma_2(\theta) = \frac{a_0^3}{128}(-2\sin 3\theta + \cos 3\theta) + c_1\sin\theta + c_2\cos\theta.$$

From the initial conditions, $\gamma_2(0) = a_2$ and $\dot{\gamma}_2(0) = 0$, we get $c_2 = a_2 - \frac{a_0^3}{128}$ and $c_1 = \frac{3a_0^3}{64}$. Therefore, $\gamma_2(\theta)$ has the form:

$$\gamma_2(\theta) = \frac{a_0^3}{128}(-2\sin 3\theta + \cos 3\theta) + \frac{3a_0^3}{64}\sin\theta + (a_2 - \frac{a_0^3}{128})\cos\theta.$$

By equating with respect to (ε^2) in (3.32) we get:

$$\begin{aligned}z_2' &= a_0\gamma_1'(\theta)\cos\theta - a_0\gamma_1(\theta)\sin\theta + a_0\gamma_1(\theta)\cos\theta \\ &= -a_0 a_1\sin\theta\cos\theta - a_0 a_1\cos\theta\sin\theta + a_0 a_1\cos^2\theta \\ &= -a_0 a_1\sin 2\theta + \frac{1}{2}a_0 a_1(1+\cos 2\theta).\end{aligned}$$

Canceling the secular term implies that $a_1 = 0$. Therefore, $z_2(\theta) = z_2(0)$, and from the condition $\int_0^{2\pi} z_2(\theta) = 0$ we get $z_2(0) = 0$ hence $z_2(\theta) = 0$, and furthermore, $\gamma_1(\theta) = 0$.

In conclusion, since $a_0 = 2\sqrt{\bar{a}}$, we have the following second order approximation

$$\begin{aligned}x(\theta) &= 2\sqrt{\bar{a}}cos(\theta) + \varepsilon^2[\frac{\bar{a}^{\frac{3}{2}}}{16}(-2\sin 3\theta + \cos 3\theta) + \frac{3\bar{a}^{\frac{3}{2}}}{8}\sin\theta + (a_2 - \frac{\bar{a}^{\frac{3}{2}}}{16})] + O(\varepsilon^3), \\ y(\theta) &= -2\sqrt{\bar{a}}sin(\theta) + \varepsilon^2[\frac{\bar{a}^{\frac{3}{2}}}{16}(-6\cos 3\theta - 3\sin 3\theta) + \frac{3\bar{a}^{\frac{3}{2}}}{8}\cos\theta] + O(\varepsilon^3), \\ z(\theta) &= 4a(\frac{1}{4}\cos(2\theta) + \frac{1}{8}\sin(2\theta) - \frac{1}{4}) + O(\varepsilon^4).\end{aligned} \tag{3.33}$$

The formula of $z(\theta)$ in the original coordinate system is given by $\varepsilon z(\theta)$. Therefore, $z(\theta)$ in the original coordinate system is given by:

$$z(\theta) = 4a(\frac{1}{4}\cos(2\theta) + \frac{1}{8}\sin(2\theta) + \frac{1}{8}) + O(\varepsilon^4) \quad ; \quad a = \varepsilon^2 \bar{a}.$$

Figure (27) shows that the oscillation center of the periodic solution of z is $z = -10^{-6}$ for $a = 10^{-6}$. From the last formula of $z(\theta)$ we have, up to $O(\varepsilon^2)$, that $\frac{1}{2\pi}\int_0^{2\pi} z(\theta) = \frac{a}{2}$ therefore the periodic solution $z(\theta)$ by the Poincare Lindstedt method oscillates around the value is $z = \frac{a}{2}$. To compare between the numerical and the analytical solutions, the solution should have the same initial points. Therefore, the analytical solution should be shifted by the value $z = -\frac{3a}{2}$, which makes the formula of $z(\theta)$ has the form

$$z(\theta) = 4a(\frac{1}{4}\cos(2\theta) + \frac{1}{8}\sin(2\theta)) - a + O(\varepsilon^4). \tag{3.34}$$

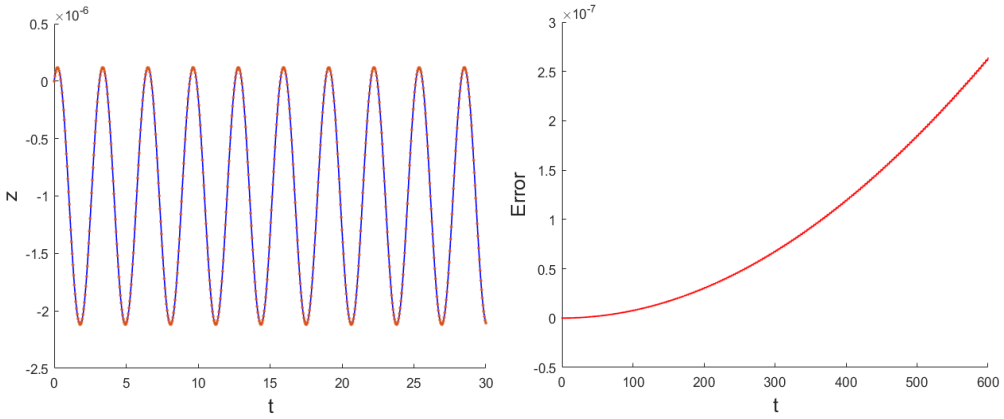

(a) (b)

Figure 30: (a) the periodic solution to $z(t)$ that correspond to the initial point $(0.002, 0, 0)$, $\varepsilon = 10^{-3}$ and $a = 10^{-6}$. The solutions were obtained numerically (blue) and analytically (dotted red) of the order (ε), which corresponds to the formula (3.34) . The two solutions seem to overlap almost perfectly on top of each other. (b) the errors of $O(\varepsilon)$.

In Figure (30a), the accuracy of the analytical solution, the red dotted graph, is of $O(\varepsilon^2)$, which is equal to the accuracy of $O(\varepsilon)$ since $z_2(\theta) = 0$ in the expansion form of $z(\theta)$. In the same figure (b), the error represent the difference between the analytical and the numerical solution with respect to time, which is of order (10^{-7}). This illustrates that the second order analytical solution is very accurate.

3.4 The Limit cycles and the chaotic attractor of the system

We have shown, using the averaging method, for a is small, there exists a periodic orbit in the neighbourhood of the origin, and moreover the second order averaging shows that this orbit is an attractor. The attracting behavior was illustrated in Poincare sections Figure (31), where it was shown that the orbit is attracted to the periodic orbit when the initial point is in the neighbourhood of the periodic orbit and the value of a corresponds to the periodic orbit. However, this attracting behaviour continues for a range of the initial radius values in the neighbourhood of the origin. In the same figure, it is illustrated that the periodic orbit is still an attractor for the initial radius $r_0 = 1$.

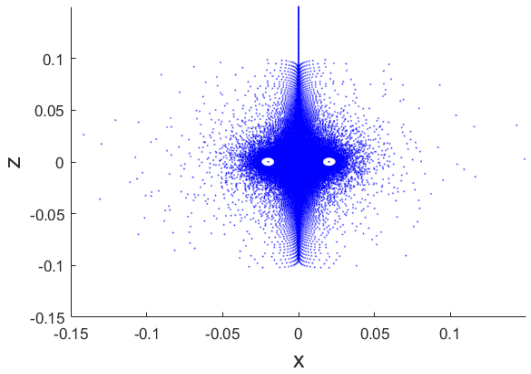

Figure 31: The Poincare sections of the orbit for $a = 0.0001$, and for the initial points $(0.02, 0, 0)$ and $(1, 0, 0)$, where the first initial point corresponds to the periodic solution for the given parameter.

Increasing the parameter a gradually shows that, for a range of the initial radius, the system has several attractors (limit cycles). We notice that the attractors have similar dynamics for a range of a values so that they are similar in shape but different in size and period, while this pattern of behaviour disappear for some other ranges of a.

In the following graphs we show a set of attractors for different values of the parameter.

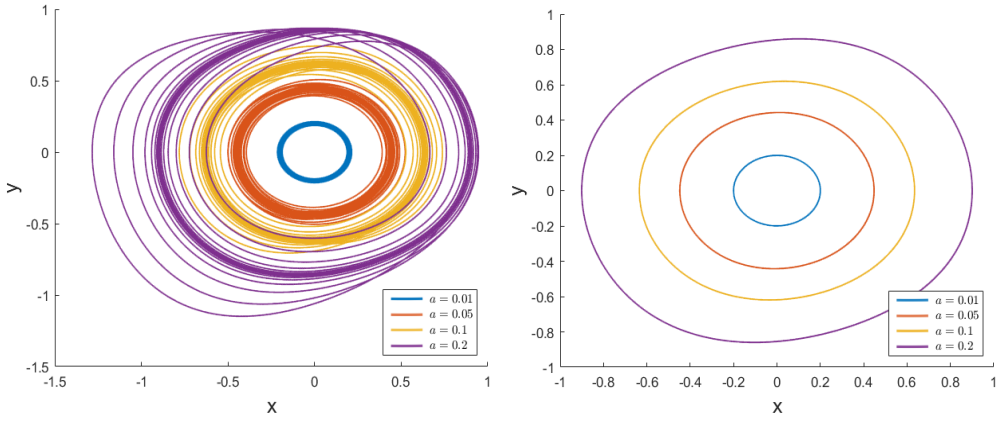

(a) (b)

Figure 32: (a) the projection of the orbit on the $xy-$plane for the initial points $(2\sqrt{a}, 0, 0)$ and a range of a values, which correspond to the periodic solutions in the neighbourhood of the origin using The averaging theorem. We notice that the plots do not show any periodic orbits since the approximation is of order (ε) which is relatively large in this case. (b) the attractors correspond to the same values of the parameter a, which show that the attractors change from a circle when a is small to an oval shape as a increases.

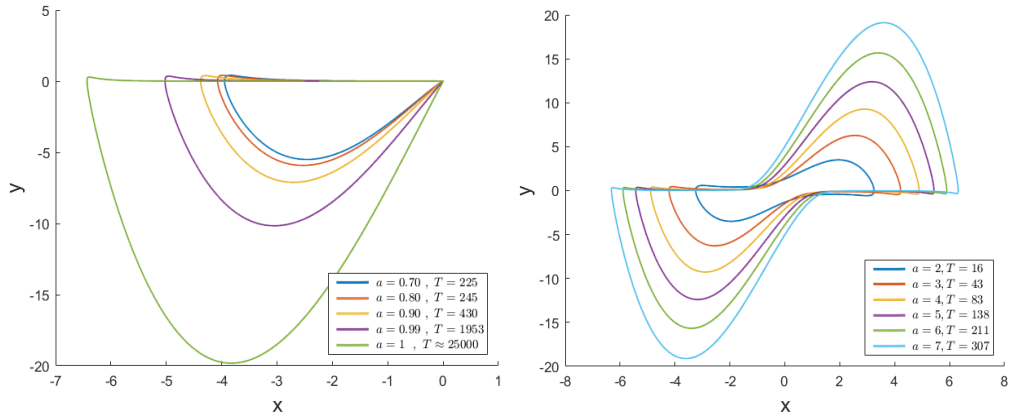

(a) (b)

Figure 33: (a) the attractor exhibits an exponential expansion for a range of a values. (b) the attractor shows a symmetrical behaviour with respect to the origin as a increases, where T represents the period of the limit cycle. The attractor expand and its period increases when a increases for a range of values of the parameter a on the $xy-$plane. The attractors are obtained from the initial point $(1,0,0)$

Remark: The symmetrical attractors of the ones in Figure (33a) are obtained for the same values of a and the initial point $(-1,0,0)$.

The Figure (33a) shows that the period of the limit cycle and its expansion increase exponentially with high rate as the parameter increases. Furthermore, the same figure, on the right, the limit cycle has the same behavior but with a low rate and moreover its projection on the $xy-$plane is symmetrical with respect to the origin.

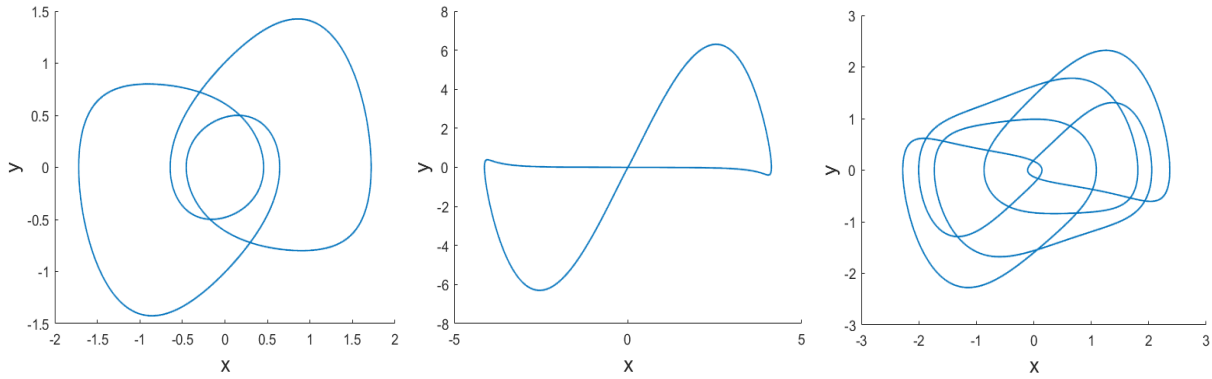

(a) (b) (c)

Figure 34: Different attractors for $a = 0.3, 0.4, 0.6$ and for the initial point $(1,0,0)$ on the $xy-$plane, which shows that a slight change in a does not lead to an expansion of the attractor, but it shows that a new attractor is created. Furthermore, the attractors are symmetrical with respect to the origin.

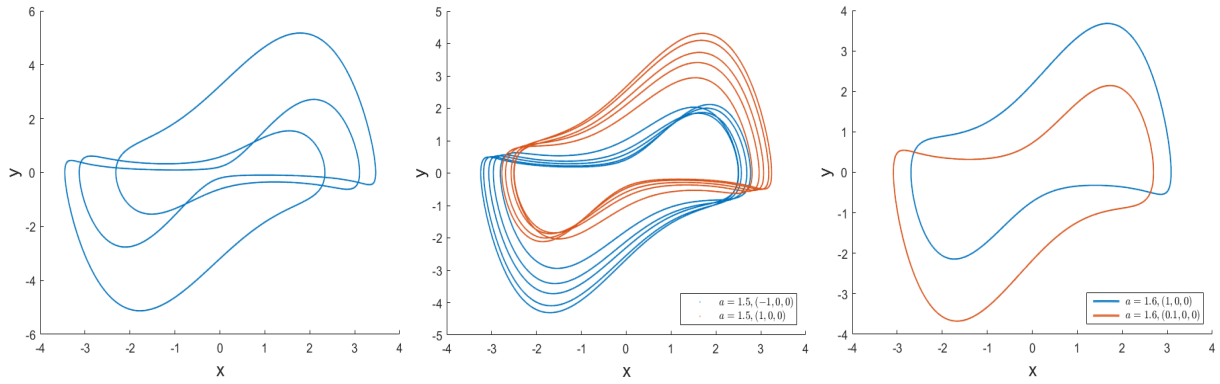

(a) (b) (c)

Figure 35: Different attractors (a) for $a = 1.4$ and for the initial point $(1,0,0)$, and (b,c) for $a = 1.5, 1.6$ and the given initial points. We notice that a slight change in a, changes the attractor from a symmetrical to an asymmetrical one. However, for two different initial points we obtain two reflectively symmetrical attractors with respect to the origin.

Furthermore, as in the case of NE9 system, the NE8 system has a cascade of period doublings that appears for a range of a values, and lead to the appearance of chaos, Figure(36a). Moreover, the chaotic behavior of the system is confirmed using the largest Lyapunov exponents, Figure(36b)

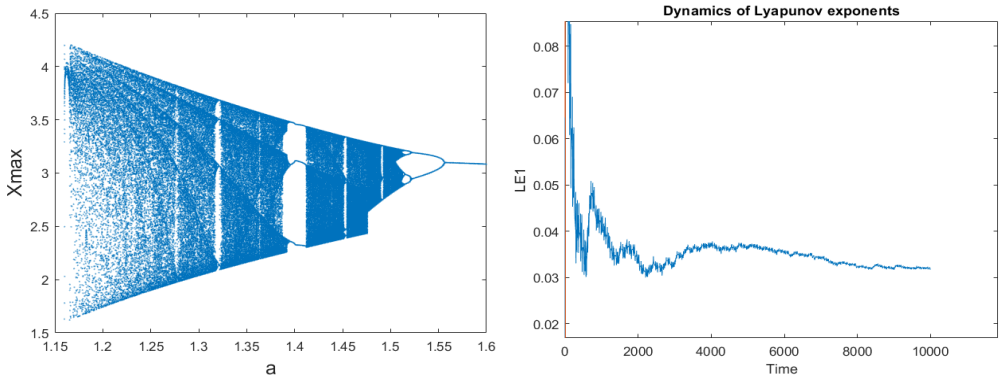

(a) (b)

Figure 36: (a) the bifurcation diagram for $a \in [1.14, 1.6]$ and for the initial point $(0, 0.1, 0)$ of NE8 system. It indicates that the system has a cascade of period doubling, which begins at approximately $a = 1.57$, and leads to chaos. (b) the change in largest Lyapunov exponent over time for the initial conditions $a = 1.3$ and $(0, 0.1, 0)$. The LE1 values are positive which confirms the occurrence of chaos.

However, a chaotic attractor appears for a values in the range $[1.1, 1.3]$, where the attractor lays on a surface in 3-dimensional space. The chaotic behavior of the attractor has been predicted by calculating the Lyapunov exponents and the Kaplan-Yorke dimension and generating some Poincare sections. For example, for the initial conditions $a = 1.3$ and $(x_0, y_0, z_0) = (0, 0.1, 0)$ the orbit corresponds to the values $LE_1 = 0.0314$, $LE_2 \approx 0$, $LE_3 = -10.2108$ and $D_{KY} = 2.0031$. The maximum value of LE and D_{KY} indicate that the motion is chaotic. Furthermore, the Poincare sections show that the orbit is dense on the surface as illustrated in Figure (37), which is another indication of the chaotic behaviour of the orbit for the given initial conditions.

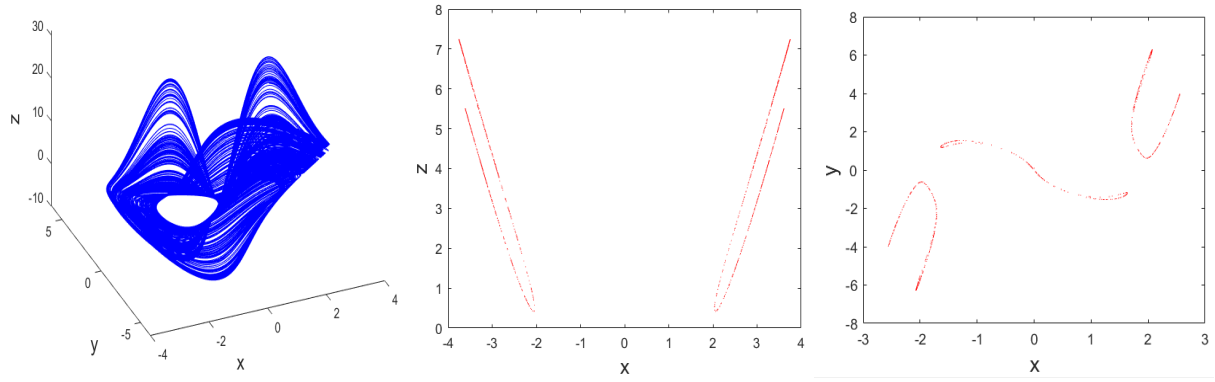

(a) (b) (c)

Figure 37: (a) the chaotic attractor on a surface in the 3-dimensional space. (b) and (c) the Poincare sections on the $xz-$ and $xy-$plane. The three graphs correspond to the initial values $a = 1.3$ and $(0, 0.1, 0)$

4 Conclusions

① We found some similarities and difference in the dynamics of the NE8 and NE9 systems at different values of the parameter a.

② For $a = 0$ we found that the $z^{+}-$axis is an axis of equilibria and that the dynamics of approaching the limit points on $z-$axis is similar in both systems given the similarity of their respective eigenvalues. However, determining analytically the limit points on the $z-$axis from the initial point is still unknown.

③ Reducing two equations of any NE system to the form $\ddot{x} + x = \varepsilon f(\dot{x}, x, y, z)$ gives the possibility of applying the averaging method to predict a periodic orbit in the neighbourhood of the origin, and studying the behaviour of the orbit in the neighbourhood of the periodic orbit. Furthermore, it allows applying the Poincare-Lindstedt method to give an analytical representation to the periodic orbit of some order of epsilon.

④ The quasi-periodic motion of the orbit in the neighbourhood of the periodic orbit is predicted from the purely imaginary conjugate eigenvalues of the averaged system. However, an analytical proof of the quasi-periodic motion of the original NE8 and NE9 systems is still needed.

⑤ We show numerically how a chaotic attractor forms in the NE9 system at some initial conditions. However, at similar initial conditions, the NE8 system has different dynamics due to the attractive nature of the periodic orbit, which does not allow for the formation of a chaotic attractor. However, the analytical proof of the formation of the chaotic attractor is still needed.

⑥ For a is small and the initial radius is large, we show that the decreasing rate of z is linear and that r behaves in a pulsating manner. Furthermore, we show, numerically, that the orbit behaves periodically for certain values of the initial conditions. These certain values satisfy the necessary conditions for periodicity, according to the Floquet theorem, but the sufficient conditions for periodicity remain unknown.

⑦ We numerically show that for some ranges of the parameter a, in the NE9 system, limit cycles were created in the phase space. However, for most values of a the numerical study shows that the orbit is unbounded from above, but an analytical proof of this dynamic is lacking.

⑧ In the NE8 system, we find groups of attractors for different ranges of the parameter a. We also find that a slight

increase in a sometimes leads to an expansion of the attractor, while at other times it changes the attractor completely. However, future numerical studies might find new attractors with a different behaviour of the orbit at different ranges of the parameter a.

⑨ The limit cycles at different ranges of a , in the NE9 system, show that the increase of the period of the cycle is approximately linear when a increases. However, the periods of the limit cycles, in the NE8 system, have two different increasing rates as a increases and a symmetrical behaviour with respect to the origin in the $xy-$plane. These dynamics have been illustrated numerically, but an analytical proof of them is still needed.

⑩ For some ranges of the parameter a, we introduce numerical evidence that a chaotic attractor forms in both systems, which is illustrated by calculating the Lyapunov exponents, the Kaplan-Yorke dimensions, the succession of period doublings bifurcation limit cycles and the Poincare sections. Moreover, the Poincare sections show that the chaotic attractor lays on a surface in the three dimensional space.

⑪ Here we give new results about the NE8 and NE9 systems that are given in this thesis:

ⓐ An analytical representation of the periodic orbit in the neighbourhood of the origin in both systems.

ⓑ A numerical illustration of the formation of the limit set and how it evolved to a chaotic attractor in the NE9 system, and showing the sensitivity of the behaviour of the orbit to the initial conditions

ⓒ In the NE9 system, $z(t)$ behaves in a zigzaging fashion and $r(t)$ in a pulsating fashion during the formation of the limit set for a is small and r_0 is larger than r_a. This behaviours of $z(t)$ and $r(t)$ were discovered in the Sprott A system (F.Verhults, private communication, 2019). Furthermore, we show that $\dot{z} \approx -a$ during the spiraling down of the orbit in the neighbourhood of $z-$axis.

ⓓ In the NE9 system, at certain initial conditions of case (c), we numerically show that the orbit behaves periodically and that for some values of the initial conditions, the necessary condition for periodicity are satisfied according to the Floquet theorem.

ⓔ We show numerically that $z(t)$ is unbounded from above for some ranges of a values and the calculations suggest that $z(t)$ grows exponentially.

ⓕ In both system, we numerically show the presence of limit cycles and the behaviour of their expansion. We also show the symmetrical dynamics of the limit cycles in the NE8 system.

ⓖ We show that the periodic orbit in the neighbourhood of the origin acts as an attractor in the NE8 system.

References

[1] Messias,M· Alisson,C. (2016). *On the formation of hidden chaotic attractors and nested invariant tori in the Sprott A system*, Nonlinear Dyn (2017) 88:807–821.

[2] Sajad Jafari, J.C. Sprott, S. Mohammad Reza Hashemi Golpayegania. Physics Letters A 377 (2013) 699–702

[3] Verhulst,F.(2000).*Nonlinear differential equations and dynamical systems*.(2nd edition).Springer Verlag Berlin Heidelberg.

[4] Verhulst,F.(2005).*Methods and Applications of Singular Perturbations* . ISBN 0-387-22966-3

[5] X. Wang, G. Chen,*Constructing a chaotic system with any number of equilibria*, arXiv:1021.5751v1, 2012.

[6] Z. Wei, Phys. Lett. A 376 (2011) 102.

[7] J.C. Sprott, Elegant Chaos: Algebraically Simple Chaotic Flows, World Scientific, 2010.

[8] W.G. Hoover, Phys. Rev. E 51 (1995) 759.

[9] H.A. Posh, W.G. Hoover, F.J. Vesely, Phys. Rev. A 33 (1986) 4253.

[10] Jafari, S., Sprott, J.C., Nazarimehr, F.: Recent new examples of hidden attractors. Eur. Phys. J. Special Top. 224, 1469–1476 (2015)

4.1 Appendix

% % This program generates the bifurcation diagram of NE9 system, Figure (23a)
% % The bifurcation diagram of NE8 system is obtained by changing the initial point and the range of a values,Figure (36a).

```
Na = 1000;
a0 = 0.548;
a1 = 0.553;
da = (a1-a0)/Na;
a = a0 + da * [0:Na]';

fsize=15;
set(gcf,'color','w');

x0 = [0.5 0 0];
X = repmat(x0,Na+1,1);
Xmax = cell(Na+1,1);

dt = 0.005;
Nsteps = 400000;

f = @(X,a) [X(:,2) -X(:,1)-X(:,2).*X(:,3)
-X(:,1).*X(:,3)+7.*X(:,1).*X(:,1)-a];

epsilon = eps;

for n=1:Nsteps

F1 = f(X,a);
F2 = f(X + dt/2*F1,a);
F3 = f(X + dt/2*F2,a);
F4 = f(X + dt*F3,a);
dXnew = dt/6*(F1 + 2*F2 + 2*F3 + F4);

Xnew = X + dXnew;

if n¿1/2 * Nsteps
ind = find((dXold(:,1)¿epsilon).*(dXnew(:,1)¡-epsilon));
for j=1:length(ind)
Xmaxind(j) = [Xmaxind(j) X(ind(j),1)];
end
end
```

```
dXold = dXnew;
X = Xnew;
end

A = [];
Xdata = [];
for j=1:Na
Xj = Xmaxj;
A = [A; a(j)*ones(size(Xj(:)))];
Xdata = [Xdata; Xj(:)];
end
plot(A,Xdata,'.','markersize',1);

xlabel('a','FontSize',fsize)
ylabel('Xmax','FontSize',fsize)
```